N O T I C E

THIS DOCUMENT HAS BEEN REPRODUCED FROM
MICROFICHE. ALTHOUGH IT IS RECOGNIZED THAT
CERTAIN PORTIONS ARE ILLEGIBLE, IT IS BEING RELEASED
IN THE INTEREST OF MAKING AVAILABLE AS MUCH
INFORMATION AS POSSIBLE

Semi Annual Status Report

NASA Grant NAG 8-564

EX-111 Thermal Emission from Hot White Dwarfs: the Suggested He Abundance-Temperature Correlation

EX-112: The Unique Emission Line White Dwarf Star GD 356

Harry L. Shipman, Principal Investigator

Physics Department, University of Delaware

PI Social Security Number: ███████████

Award Amount: $20,000

Award Dates: December 1, 1985 - December 1, 1986
Period Covered: December 1, 1985 - June 1, 1986

_____   8/27/86
PI Signature   _____
                                 Date

EXOSAT observations of four of the five white dwarfs which we had obtained observing time for were obtained in December 1985 and February 1986. The stars observed were WD1031-115, WD0004+330, WD0109-264, and WD1615-154. Counting rates were unexpectedly low, indicating that these objects have a substantial amount of x-ray absorbing matter in their photospheres. Analysis of these data is continuing. EXOSAT was not able to obtain data on the unusual magnetic white dwarf GD 356 before it ceased operations in March 1986.

The research on this grant took an unexpected turn with the discovery of 9.25 minute pulsations in the DA white dwarf V471 Tauri. I worked closely with the Goddard group (K. Jensen, R. Petre, J. Swank) on the preliminary interpretation of this object. A paper describing our results has been accepted by the Astrophysical Journal Letters and a preprint is appended to this report. In February 1986 a second observation of this star confirmed the existence of the 9.25 minute pulsations. Our analysis of this star is hampered by the sparseness of the grid of model atmospheres which is available, and a finer model grid will be calculated shortly.

Another unexpected turn of events came with the availability of EXOSAT data on the hot white dwarf H1504+65. This unique, freakish object is probably the only object we know of which has neither hydrogen nor helium in its photosphere. I was second author and principal data analyst on a long paper which has been accepted by the Astrophysical Journal.

In a related paper, my graduate student Peter Thejll and I analyzed the existing data on the white dwarf Sirius B to see what constraints from other data can be placed on the properties of this star. EXOSAT has obtained some spectra for Sirius B. This paper has been accepted for publication by the Publications of the Astronomical Society of the Pacific.

List of Publications

K. A. Jensen, J. H. Swank, R. Petre, E.F. Guinan, E.M. Sion, and H.L. Shipman*, "EXOSAT Observations of V471 Tauri: I. A 9.25 Minute Pulsation from the White Dwarf and Orbital Phase Dependent X-Ray Absorption Dips," Astrophysical Journal Letters, in press.

J. A. Nousek, H. L. Shipman*, J. B. Holberg, J. Liewbert, S. H. Pravdo, N. E. White, and P. Giommi, "H1504+65: An Extraordinarily Hot, Compact Star Devoid of Hydrogen and Helium," Astrophysical Journal, in press.

P. A. Thejll* and H. L. Shipman,* "Temperature, Radius, and Rotational Velocity of Sirius B," Publications of the Astronomical Society of the Pacific, in press.

H1504+65: An Extraordinarily Hot Compact Star Devoid

of Hydrogen and Helium

J.A. Nousek[1,2]

Department of Astronomy, The Pennsylvania State University

Harry L. Shipman[2]

Department of Physics, University of Delaware

J.B. Holberg[5] and James Liebert[5]

Lunar and Planetary Laboratory and Steward Observatory,

University of Arizona

Steven H. Pravdo[3,4]

The Jet Propulsion Laboratory

and

N.E. White[6] and Paolo Giommi[6]

European Space Operations Center

Abstract

We report the optical identification of the bright soft X-ray source H1504+65, originally discovered by the <u>HEAO-1</u> A-2 Low Energy Detectors. The optical counterpart, selected on the basis of an objective prism plate from the Burrell Schmidt, exhibits a steep, virtually featureless, continuum from optical wavelengths through the ultraviolet. <u>EXOSAT</u> observations of the object confirm the identification and provide important soft X-ray spectral information. <u>IUE</u> and <u>Voyager 2</u> spectra, combined with ground based spectroscopy, reveal the continuum extends without inflection out to the Lyman limit, where interstellar absorption cuts it off. The energy distribution is characterized by a single power law of the form $F_\lambda \propto \lambda^{-4}$ from 912 Å to 8000 Å. At high resolution the spectrum is remarkably featureless except for a broad O VI absorption feature at $\lambda 3494.7$ and C IV in absorption at 3934 Å and emission at 4658 Å. The presence of O VI is supported by an O VI resonance feature seen in the <u>Voyager</u> data. Weak Lyman alpha absorption is detected in small aperture <u>IUE</u> spectra, which is consistent with interstellar absorption.

The soft X-ray data, which are not consistent with any published models for degenerate stars having predominantly H or He compositions, suggest that H1504+65 is a metal rich, near degenerate object, of very high temperature. Qualitative considerations based on the optical spectra, the observed ultraviolet spectrum, and interpretations of the X-ray fluxes indicate that it is definitely hotter than PG1159-035 and similar objects. Our best estimate of the temperature is 160,000 K with considerable uncertainty (roughly 30,000 K) since no model or

black body is consistent with the available data. Evolutionarily, it
is similar to the central stars of planetary nebulae, of recent origin,
and currently in a state of rapid thermal evolution.

SUBJECT HEADINGS: Spectrophotometry – stars: individual (H1504+65) –

stars: white dwarfs – ultraviolet: spectra –

X-rays: sources

Abstract

We report the optical identification of the bright soft X-ray source H1504+65, originally discovered by the HEAO-1 A-2 Low Energy Detectors. The optical counterpart, selected on the basis of an objective prism plate from the Burrell Schmidt, exhibits a steep, virtually featureless, continuum from optical wavelengths through the ultraviolet. EXOSAT observations of the object confirm the identification and provide important soft X-ray spectral information. IUE and Voyager 2 spectra, combined with ground based spectroscopy, reveal the continuum extends without inflection out to the Lyman limit, where interstellar absorption cuts it off. The energy distribution is characterized by a single power law of the form $F_\lambda \propto \lambda^{-4}$ from 912 Å to 8000 Å. At high resolution the spectrum is remarkably featureless except for a broad O VI absorption feature at λ3494.7 and C IV in absorption at 3934 Å and emission at 4658 Å. The presence of O VI is supported by an O VI resonance feature seen in the Voyager data. Weak Lyman alpha absorption is detected in small aperture IUE spectra, which is consistent with interstellar absorption.

The soft X-ray data, which are not consistent with any published models for degenerate stars having predominantly H or He compositions, suggest that H1504+65 is a metal rich, near degenerate object, of very high temperature. Qualitative considerations based on the optical spectra, the observed ultraviolet spectrum, and interpretations of the X-ray fluxes indicate that it is definitely hotter than PG1159-035 and similar objects. Our best estimate of the temperature is 160,000 K with considerable uncertainty (roughly 30,000 K) since no model or

I. INTRODUCTION

The soft X-ray sky is a relatively recently explored portion of the electromagnetic spectrum (E $\sim$ 0.1-1 keV, $\lambda \sim$ 10-100 Å). The HEAO-1 A-2[7] experiment Low Energy Detectors (LED) performed the most sensitive

---

[7] The A-2 experiment on HEAO-1 was a collaborative effort lead by E. Boldt of Goddard Space Flight Center (GSFC) and G. Garmire of Penn State with collaborators at GSFC, Penn State, The Jet Propulsion Laboratory and the University of California, Berkeley.

---

all sky survey for point sources of X-rays in this energy range (Nugent et al. 1983). Of the 114 sources cataloged, half were previously unknown.

We are attempting a systematic effort to identify these brightest sources, in the hopes that these bright objects are the closest or most conspicuous members of interesting classes. Unfortunately the HEAO-1 data alone can not precisely locate the X-ray source but have an uncertainty in position (error box) of order 0.3 square degrees.

H1504+65 is the seventh brightest source in the 0.25 keV band (0.18-.44 keV) observed by HEAO-1, but was undetected at 1 keV (0.44-2.8 keV) (Nugent et al. 1983). Objective prism plates taken with the 0.6 m Burrell Schmidt at Kitt Peak of the H1504+65 error box revealed a faint ($m_V \sim$ 16), extremely blue continuum object at (α, δ = (1950.0) = (15^h 01^m 23.1^s, +66° 24' 09"). Moderate resolution spectroscopy using the Palomar 1.5 m reflector and the Penn State 1.6 m reflector confirmed the blue continuum, but found no evidence for emission or absorption lines. High resolution optical spectroscopy using the 2.1m

Steward Observatory reflector have placed stringent limits on the presence of absorption or emission features from 4000 to 5000 A, but did show some features from C IV and O VI. Ultraviolet spectroscopy from the International Ultraviolet Explorer (IUE) also found an extremely blue continuum, and small-aperture spectroscopy indicated the presence of interstellar Lyman alpha. Voyager observations have shown that the continuous slope extends without break to the Lyman limit, and also demonstrated the presence of O VI 1032. EXOSAT observations, using the Channel Multiplier Array (CMA), have confirmed the identification of the X-ray source with the optical candidate and provided important soft X-ray spectral information by using several filters.

In the following sections we describe the optical observations (§II), the ultraviolet observations (§III), the X-ray observations (§IV), interpret these observations (§V) and discuss our understanding of the nature of H1504+65 (§VI).

II. OPTICAL OBSERVATIONS

a) Objective Prism

An objective prism IIIa-J plate exposure of 75^m was taken of the
H1504+65 error box on 1982 April 24, using the 0.6 m Burrell Schmidt
with thin prism at Kitt Peak National Observatory by A. Wasilewski as
part of a Visiting Astronomer program with J.A.N. and D. Weedman. Care-
ful search of the H1504+65 error box by Dr. Weedman revealed a dramati-
cally blue continuum object at $\alpha,\delta(1950) = 15^h01^m23^s.1, +66°24'09"$
(Figure 1). No emission or absorption features were apparent on the
spectrum covered on the plate ($\sim$3600-5400 Å) down to a limit of approx-
imately 150 Å equivalent width. The stellar image shows no proper mo-
tion, with an upper limit of 0.06" yr^{-1} (Giclas, private communication).

b) Low Resolution Spectroscopy

Optical spectroscopy of the blue candidate was performed at the 1.6
m reflector of the Black Moshannon Observatory (BMO) of Penn State by
JAN and L. Takalo and at the 1.6m reflector of the Palomar Observatory
by SHP and F. Marshall. The BMO observations on 1983 July 13 using a
fiber coupled SIT spectrograph (Ramsey, Nations and Barden 1981) total-
led 3000 seconds and covered the spectral range 4500-8100 Å with a reso-
lution of 25 Å. The Palomar observations on 1982 May 25 employed a SIT
Cassegrain spectrograph, totalled 1800 seconds and covered the spectral
range 3500-6500 Å at a resolution of 15 Å.

These observations found a steep, blue, featureless continuum
(Figure 2) with a magnitude of 16.1 at 5000 Å. In particular the upper
limit to the equivalent width of any absorption or emission is 6 Å at Hα and
5 Å at Hβ.

c) High Resolution Spectroscopy

Higher resolution observations of H1504+65 have been obtained by

J.B.H. and J.L. with the Steward Observatory 2.3 m reflector and the Multiple Mirror Telescope. Initial 2.3 m observations were performed on 1985 February 12 using the photon counting Reticon detector system with an ultraviolet – sensitive image tube. An 832 line mm^{-1} grating was employed which achieved an effective resolution of ~2.25 Å over the 3900 Å to 5000 Å region. A total effective observation time of 1320 s yielded a steeply rising continuum[8] with no apparent features.

---

[8]It is worth emphasizing that, over the optical spectral range of 4000-5000 Å, this star more closely resembles a continuous spectrum than any other star we have observed at this spectral resolution with data of similar quality, including at least 1000 PG Survey stars. Only DC white dwarfs cooler than 12,000 K exhibit fewer apparent features. Of course some central stars of planetary nebulae are assigned "continuous" spectra but generally the quality of the observations is not as good with the stellar spectrum being complicated by overlying nebular emission.

In particular there was no evidence for either Hγ or Hδ, the upper limit for the former being 0.3 Å.

A second high resolution spectrum was obtained with the Arizona/ Smithsonian 4.5 m Multiple Mirror Telescope on 31 March (U.T.). The use of a similar 832 line mm^{-1} grating afforded coverage of 4050-4950 Å at 1 Å resolution. The detector system consisted of a blue-sensitive image tube and photon counting Reticon. However, the larger telescope aperture and better sensitivity of the detector near 5000 Å allowed better coverage of the 4500-5000 Å region in particular than for the 2.3 m scan. In agreement with the former, there was no con-

clusive evidence for broad or narrow stellar absorption features.
Upper limits for Hγ, Hβ, He II λ4686 and He II λ4540 are 0.5 Å or less
(Fig. 3a). In particular, the "absorption trough" due to blends of
C IV λ4658 and He II λ4686, so characteristic of the so-called PG1159
spectroscopic group (Wesemael, Green and Liebert 1985) is absent.[9]

---

[9]The only conceivable absorption here consists of extremely broad,
shallow line wings with virtually no cores. Such a possible feature
appears near 4500 Å as well, but this has no logical identification.

---

convincingly in both independently-reduced array spectra. This line
appears marginally resolved, with a FWHM width of about 2.8 Å. The
corresponding C IV λ4441 emission line also seen in some PG1159 stars
is at best marginally present in this spectrum.

A follow up 2.3 m observation of H1504+65 was performed on 28 May
1985 with the same instrumentation but with the grating tilted so as to
cover the 3200 to 4300 Å region. This spectrum, with an effective
integration time of 1380 s, is shown in Figure 3b. A broad absorption
feature exhibiting a narrow central emission reversal is clearly
apparent. We identify this feature as due to O VI λ3434.7 and note the
possible presence of weaker features due to the same ion at 3314 Å and
3622 Å. A broad but weak C IV feature is also evident at 3934 Å as
well as unidentified absorption blends blueward of that position.

Using the CIV 4658 Å emission feature as a fiducial we determine
a heliocentric radial velocity of 0 ± 15 km/s for H1504+65.

III. ULTRAVIOLET OBSERVATIONS

a) IUE

Despite its faint optical flux ($V \sim 16.24$) the presence of X-ray flux and the extremely blue optical continuum encouraged us to request ultraviolet observations of the candidate using IUE (Boggess et al. 1978). Low dispersion spectra (resolution ~ 6 Å) were obtained by J.A.N. on 1983 June 13 and 1984 October 31 with both the long and short wavelength cameras, covering the wavelength range from 1150-3200 Å.

The ultraviolet spectra show no sign of variability between observations. As in the optical, the ultraviolet continuum is steeply, and smoothly rising toward short wavelength (Figure 4). Because of the broad geocoronal emission, the standard, large aperture spectra provide only rather weak constraints on the presence or absence of Lyman alpha. Consequently, a small aperture spectrum, SWP 25323, was obtained by H.L.S. on February 26, 1985, revealing a modest Lyman alpha absorption feature. Because the sensitivity of the IUE spectrograph falls steeply shortward of Lyman alpha, uncertainties in continuum placement limit our ability to measure the equivalent width of this feature. Our best estimate is that the equivalent width is 5.7 ± 1 A.

Except at Lyman alpha there are no emission or absorption features in the ultraviolet exceeding 20% of the continuum. Possible weak absorption features may be present near 1258, 1290, and 1300 Å with equivalent widths near 2 Å. No sign of interstellar extinction is found near 2200 Å.

b) Voyager 2

In addition to IUE, far UV observations of H1504+65 were also obtained with the ultraviolet spectrometers on board Voyager 2

(Broadfoot et al. 1977 and 1981). These observations covered the
period 1984 November 19 to 1984 December 28. During this period 7684
s of high rate data (3.84 s/spectra) and 9215 s of low rate (575 s/
spectra) data were obtained with the source near the center of the
field of view. The data were reduced in a manner similar to that
described in Drilling, Holberg, and Schoenberner (1984) and employed
the calibration of Holberg et al. (1982).

Resultant 912 to 1083 A fluxes are shown in Figure 2. These data,
which are obtained at 9.26 A per channel, have an effective spectral
resolution of $\sim$ 25 Å. At t. 's relatively low resolution a statistical-
ly significant absorption feature centered on a wavelength of 1032 A
is apparent. In light of the presence of O VI in the visual spectra we
feel secure in identifying this feature as a blend of the resonant
O VI doublet lines $\lambda\lambda$ 1031.9 and 1037.6. A weaker, but still signifi-
cant feature, is also present at $\sim$ 977 Å.

IV. X-RAY OBSERVATIONS

a) HEAO-1 A-2 Low Energy Detectors (LED's)

H1504+65 was discovered by the HEAO-1 LED experiment as a point
source of X-rays in the 0.18-0.44 keV band. The HEAO-1 LED's were
collimated thin window proportional counters which scanned along lines
of constant ecliptic latitude once every 33 minutes, and stepped along
the ecliptic equator at a rate of $1°$ per day (Rothschild et al. 1979).
In this way virtually the entire sky was surveyed for X-ray sources
with a positional resolution of approximately $0.3° \times 1°$.

HEAO-1 scanned H1504+65 in 1977 December and 1978 May. The
0.18-0.44 keV X-ray intensity in the two observations showed no sign
of variability and were consistent with a count rate of 5.9 ± 1.4
counts s^{-1}. No source was detected at this position in the 0.44-2.8
keV band down to a 2σ limit of 1.7 counts s^{-1}.

The spectrum of pulse heights induced in the LEDs by H1504+65 was
very soft, confined to the lowest three pulse height channels. Within
photon counting statistics the spectral shape is the same as that
observed in HZ 43, a very low energy black body spectrum, $T < 10^6$ K,
with no indication of absorbing gas.

The determination of absolute fluxes from the HEAO-1 data is
rather model dependent. For illustrative purposes, we have determined
the flux in the 0.18-0.44 keV band for a 150,000 K black body input
spectrum and a hydrogen column density of 10^{20} cm^{-2}, to be $7.4 \pm 1.8 \times$
10^{-12} erg cm^2 s^{-1}. However we note that since the spectrum is very
soft, this number should be regarded with care in any future atmospher-
ic modeling efforts. The need for caution in modeling the X-ray
counting rates for sources of this type has been known for some time

(Broadfoot et al. 1977 and 1981). These observations covered the
period 1984 November 19 to 1984 December 28. During this period 7684
s of high rate data (3.84 s/spectra) and 9215 s of low rate (575 s/
spectra) data were obtained with the source near the center of the
field of view. The data were reduced in a manner similar to that
described in Drilling, Holberg, and Schoenberner (1984) and employed
the calibration of Holberg et al. (1982).

Resultant 912 to 1083 A fluxes are shown in Figure 2. These data,
which are obtained at 9.26 A per channel, have an effective spectral
resolution of $\sim$ 25 Å. At this relatively low resolution a statistical-
ly significant absorption feature centered on a wavelength of 1032 A
is apparent. In light of the presence of O VI in the visual spectra we
feel secure in identifying this feature as a blend of the resonant
O VI doublet lines $\lambda\lambda$ 1031.9 and 1037.6. A weaker, but still signifi-
cant feature, is also present at $\sim$ 977 Å.

(Shipman 1976, Kahn et al. 1984).

b) EXOSAT Low Energy Experiment CMA

The EXOSAT Low Energy Experiment (LE) observed H1504+65 on 1984
March 28 using a channel multiplier array (CMA) at the focus of an
imaging telescope (de Korte et al. 1981). It detected a bright X-ray
source coincident, within the 10" error radius, with the blue optical
candidate discussed in §II, confirming the X-ray source identification.
The CMA has no intrinsic spectroscopic capability, but observations
were conducted through three different filters, allowing inference of
spectral shape by the variation in observed intensity. The filters
used were the thin Lexan (Lexan 3000), Parylene-N with aluminum (Al),
and boron on polypropylene (B). The observed rates from H1504+65 were
$6.97 \pm .04$, $0.47 \pm .02$ and $0.017 \pm .002$ counts s^{-1}, for the Lexan 3000,
Al and B filters respectively.

FFT analysis of the thin Lexan photon arrival times showed no
evidence for periodicity. The upper limit to variation is 5% for
timescales between one second and one hour. Rates seen in the other
bands similarly show no evidence of periodicity.

V. INTERPRETATION

While there is a considerable amount of data available on this
star, there is no single model in the literature which fits it all,
and the discrepancies between model and observation, particularly in
the X-ray spectral region, are extreme rather than marginal. This
suggests that the chemical composition of H1504+65 is rather unlike the
composition of existing models (i.e., pure H, pure He, or solar
composition), though further modeling would be necessary in order to
demonstrate this suggestion conclusively. Our inability to fit models
to data makes it necessary to appeal occasionally to qualitative or
semi-quantitative arguments. In this section, we discuss the inter-
pretation of the data, wavelength region, and in section VI we discuss
our overall interpretation of this highly unusual object.

a) Optical Observations

The most striking feature of the optical spectra is the absence of
H I, He II lines, lines which are found in all other degenerates and
subdwarfs, and in planetary nebula nuclei with sufficiently high
quality spectra. The upper limits of 0.3 Å (for Hγ and Hδ) and 0.5 Å
(for Hβ, He II 4686, and He II 4540) dictate that if this object has a
H- or He-rich atmosphere, it is considerably hotter than the highest
temperature models in the grids of Wesemael et al. (1980) or Wesemael
(1981) -- 200,000 (log g = 7) for the H-rich models and 150,000 for
the He-rich models (this is the highest temperature model for which
Wesemael quotes He line strengths).

A purely qualitative analysis, in comparison with the PG 1159
objects and with the hottest main sequence stars, supports the idea of
an extreme temperature for this object. The hottest O-type stars like

(Shipman 1976, Kahn et al. 1984).

b) EXOSAT Low Energy Experiment CMA

The EXOSAT Low Energy Experiment (LE) observed H1504+65 on 1984 March 28 using a channel multiplier array (CMA) at the focus of an imaging telescope (de Korte et al. 1981). It detected a bright X-ray source coincident, within the 10" error radius, with the blue optical candidate discussed in §II, confirming the X-ray source identification. The CMA has no intrinsic spectroscopic capability, but observations were conducted through three different filters, allowing inference of spectral shape by the variation in observed intensity. The filters used were the thin Lexan (Lexan 3000), Parylene-N with aluminum (Al), and boron on polypropylene (B). The observed rates from H1504+65 were $6.97 \pm .04$, $0.47 \pm .02$ and $0.017 \pm .002$ counts s^{-1}, for the Lexan 3000, Al and B filters respectively.

FFT analysis of the thin Lexan photon arrival times showed no evidence for periodicity. The upper limit to variation is 5% for timescales between one second and one hour. Rates seen in the other bands similarly show no evidence of periodicity.

Zeta Puppis, with T(eff) = 46,000 ± 4,000 K (de Jager 1980) have both C III and C IV lines, as do the hottest Wolf-Rayet stars which show carbon. H1504 has only C IV lines. This type of ionization argument is relatively independent of chemical composition, and hence does not require that we assume a H- or He-dominated atmosphere.

A closer, and more instructive, comparison can be made between H1504 and the PG 1159 objects. Sion, Liebert, and Starrfield (1985) have discussed similar O VI and C IV features in five members of this class of objects, including PG 1159-035 itself. In the visual the spectra of PG 1159 objects are characterized by steep, nearly Rayleigh-Jeans continua with broad features due to He II, C IV, possibly Si IV, and no H I Balmer lines (Wesemael, Green, and Liebert 1985). In the optical ultraviolet Sion, Liebert, and Starrfield find that O VI 3434.7 and C IV 3934 are strong features in the PG 1159 objects they examined. Both are evident in our data, but they are substantially weaker in H1504. Further, the C IV 3689 line, strong in the PG 1159 objects, is absent in H1504. Because it comes from a different multiplet than the C IV 3934 line, the difference in the 3934/3689 line ratios (> 1 in PG 1159 objects and < 1 in H1504) is not a definitive indication of a misidentification of the C IV 3934 line, but it is an indication of the need for further modeling and investigation of the C spectrum. The weakness of the C IV and O VI lines which we do detect could conceivably be due to an underabundance of O VI and C IV relative to the PG objects, but is is more likely due to a significantly higher temperature. Additionally, the presence of He II in PG 1159 and its absence in H1504 suggests that if the atmosphere of H1504 is He dominated, or has a similar He content to that of PG 1159, that H1504 is considerably

hotter so that He is more ionized (to He III).

The similarity between H1504 and the PG objects does not extend to the IUE spectral region, but again a higher temperature for H1504 seems to be the cause. Other dissimilarities (the absence of C IV 1550 and N V 1240) could be either temperature or abundance effects.

The O VI 3434.7 line found in H1504 is at least as strong as found in PG 1159 objects. Note that the width of this profile is also at least as great as seen in PG 1159. While here as with other data a model atmosphere analysis will be required for definitive results, this profile similarity suggests some statements about surface gravity. Wesemael, Green and Liebert (1985) estimated log g = 7 for the PG 1159 group based on comparison of the He II lines with models. We believe that the similarity in the O VI profile of H1504+65 indicates a correspondingly high surface gravity.

b) Ultraviolet Continuum

Figure 2 demonstrates that the continuum rises very steeply into the ultraviolet. The SWP data alone, as well as the SWP data plus the visual point, fit a relationship of $H_\lambda \propto \lambda^{-4.1\pm0.1}$ (which is the same as $H_\nu \propto \nu^{2.1}$). The LWP and Voyager data are both noisier and are somewhat offset from the SWP data; in our view, they are consistent with a power law with a spectral index of 4.1 ± 0.1. (Since IUE fluxes are generally quoted in wavelength units, we define a spectral index x by the equation $H_\lambda \propto \lambda^{-x}$.

One can take two approaches to interpreting these continuum slopes. Calibration uncertainties are the smallest if one only considers the data from a particular spectrograph on a particular instrument, and the one with the greatest leverage and quality here is the

Zeta Puppis, with T(eff) = 46,000 ± 4,000 K (de Jager 1980) have both C III and C IV lines, as do the hottest Wolf-Rayet stars which show carbon. H1504 has only C IV lines. This type of ionization argument is relatively independent of chemical composition, and hence does not require that we assume a H- or He-dominated atmosphere.

A closer, and more instructive, comparison can be made between H1504 and the PG 1159 objects. Sion, Liebert, and Starrfield (1985) have discussed similar O VI and C IV features in five members of this class of objects, including PG 1159-035 itself. In the visual the spectra of PG 1159 objects are characterized by steep, nearly Rayleigh-Jeans continua with broad features due to He II, C IV, possibly Si IV, and no H I Balmer lines (Wesemael, Green, and Liebert 1985). In the optical ultraviolet Sion, Liebert, and Starrfield find that O VI 3434.7 and C IV 3934 are strong features in the PG 1159 objects they examined. Both are evident in our data, but they are substantially weaker in H1504. Further, the C IV 3689 line, strong in the PG 1159 objects, is absent in H1504. Because it comes from a different multiplet than the C IV 3934 line, the difference in the 3934/3689 line ratios (> 1 in PG 1159 objects and < 1 in H1504) is not a definitive indication of a misidentification of the C IV 3934 line, but it is an indication of the need for further modeling and investigation of the C spectrum. The weakness of the C IV and O VI lines which we do detect could conceivably be due to an underabundance of O VI and C IV relative to the PG objects, but is is more likely due to a significantly higher temperature. Additionally, the presence of He II in PG 1159 and its absence in H1504 suggests that if the atmosphere of H1504 is He dominated, or has a similar He content to that of PG 1159, that H1504 is considerably

IUE SWP spectrograph.. Fig. 6 compares our observed value to those given by models; the uncertainty in our observed value includes equal contributions of 5% from photon statistics and 5% from the uncertainty in the IUE calibration. It is clear that the observed "super-infinite" spectral index is, even considering the substantial uncertainties from calibration, higher than those produced by the H-rich models of Wesemael et al. (1980), and is hotter than the Wesemael's (1981) hottest He model with T(eff) = 150,000 K. A blackbody "fit" gives a nominal 2-sigma lower limit to the temperature of 500,000 K; this limit should not be taken too seriously.

Another approach is to use the widest baseline possible, where good data exists. Comparison of the Voyager and optical data gives a spectral index of 4.3; comparison of the IUE SWP data and the optical gives a spectral index of 4.0. UV/optical spectral indices from the Wesemael models are about 0.08 higher than the UV indices plotted in Fig. 6; one comes up with a similar conclusion, that neither the H-rich nor the He-rich Wesemael models fit the data, that the star is very hot, and that it is hotter than the PG 1159 objects.

c) Lyman Alpha

The small-aperture SWP spectrum did show a Lyman alpha feature. This is clearly interstellar. If it were stellar, the indicated effective temperature from the Wesemael models would be $(80-100) \times 10^3$ K, not an implausible value, but then the equivalent width of Hβ or Hγ would be at least 1.8 A for a continuum 30 A from line center. A relationship between the equivalent width of interstellar Lyman alpha and the interstellar column density N_H is given by Morton (1967) as

$$W(A) = 7.31 \times 10^{-10} (N_H)^{1/2}.$$

While the rapidly changing sensitivity of the IUE, and the somewhat noisy small aperture spectrum, make measurement of W uncertain, the observed value of $W = 5.7 \pm 1$ A leads to an interstellar column density of $(0.6 \pm 0.2) \times 10^{20}$ atoms cm^{-2}. While the fits to the X-ray data reveal no clear choice of model or N_H (see below), this value is reasonably consistent with the X-ray data, particularly the very soft data point from EXOSAT.

d) HEAO-1

There are a fair variety of approaches to analyzing the X-ray emission from individual white dwarf stars (see, e.g., Shipman 1976, Auer and Shipman 1977, Malina, Basri, and Bowyer 1982, Martin et al. 1982, Kahn et al. 1984, Holberg, Wesemael, and Hubený 1984, Petre, Shipman, and Canizares 1985). The difficulty faced by all these authors is that the number of spectrally independent data points in the X-ray band is typically one or, at most a few, low resolution measurements of the integrated flux. Balancing this difficulty is the tremendous leverage offered by the extremely steep dependence of the X-ray flux on the physical parameters of interest, usually T(eff) and n(He), and its virtual independence of surface gravity.

We face an additional difficulty in analyzing the HEAO-1 data in that the detector calibration is a strong function of the shape of the assumed incident spectrum. For ultrasoft sources like white dwarf stars, the convolution of the steeply falling incident spectrum with the sharply rising detector response means that virtually all the counts come from the softest energy which the instrument can detect. This means that the distribution observed in the detector is unchanged over a wide range of assumed incident spectra, but the detector

<u>IUE</u> SWP spectrograph.. Fig. 6 compares our observed value to those given by models; the uncertainty in our observed value includes equal contributions of 5% from photon statistics and 5% from the uncertainty in the <u>IUE</u> calibration. It is clear that the observed "super-infinite" spectral index is, even considering the substantial uncertainties from calibration, higher than those produced by the H-rich models of Wesemael et al. (1980), and is hotter than the Wesemael's (1981) hottest He model with $T(eff) = 150,000$ K. A blackbody "fit" gives a nominal 2-sigma lower limit to the temperature of 500,000 K; this limit should not be taken too seriously.

Another approach is to use the widest baseline possible, where good data exists. Comparison of the <u>Voyager</u> and optical data gives a spectral index of 4.3; comparison of the <u>IUE</u> SWP data and the optical gives a spectral index of 4.0. UV/optical spectral indices from the Wesemael models are about 0.08 higher than the UV indices plotted in Fig. 6; one comes up with a similar conclusion, that neither the H-rich nor the He-rich Wesemael models fit the data, that the star is very hot, and that it is h ter than the PG 1159 objects.

c) Lyman Alpha

The small-aperture SWP spectrum did show a Lyman alpha feature. This is clearly interstellar. If it were stellar, the indicated effective temperature from the Wesemael models would be $(80-100) \times 10^3$ K, not an implausible value, but then the equivalent width of Hβ or Hγ would be at least 1.8 A for a continuum 30 A from line center. A relationship between the equivalent width of interstellar Lyman alpha and the interstellar column density N_H is given by Morton (1967) as

$$W(A) = 7.31 \times 10^{-10} (N_H)^{1/2}.$$

efficiency changes dramatically. For example, the soft X-ray flux inferred from a given count rate changes by a factor of twenty when the assumed incident spectrum is changed from a 100,000 K black body to a 200,000 K black body. Hence we can not infer a temperature or even a flux in the soft X-ray band without knowledge from other data of the incident spectral shape.

To escape this extreme model dependency we have chosen to form a completely empirical quantity, $[L_x/L_v]$, based on the ratio of X-ray to optical flux between H1504 and HZ 43. We define

$$[L_x/L_v] = \frac{[f_x/f_v]_{H1504+65}}{[f_x/f_v]_{HZ43}} \, ,$$

where the f's are the observed fluxes. To first order the ratio f_x/f_v takes out differences in distance and stellar radius, so $[L_x/L_v]$ should be one, if H1504 and HZ 43 have the same spectrum (HZ 43 was selected as a reference because it was well observed optically and by HEAO-1 and EXOSAT). $[L_x/L_v]$ is found to be 8.1 ± 2, indicating that H1504 has a spectrum proportionately emitting more X-rays than HZ 43.

To achieve quantitative temperature estimates it is necessary to invoke models, but by making the comparisons in terms of $[L_x/L_v]$ we hope that model inadequacies will also cancel to first order. We used a 60,000 K pure hydrogen model to represent the spectrum of HZ 43. Uncertainties in the temperature or spectrum of HZ 43 affect this scheme, but by a small amount; a 3000 K change in the temperature of HZ 43 changes the value of $[L_x/L_v]$ by only 1.5, a small effect in light of the tremendous leverage offered by observations of thermal X-rays.

An additional correction to be made is that for interstellar absorption. Nugent et al. (1983) in Fig. 4, give corrections which

can be applied to black bodies. In those cases where we tried to fit models to the data, we used the black body temperature which came closest to fitting the model spectrum in the 100-200 eV region.

Now consider fitting the data for various possible chemical compositions. If H1504+65 were H-rich, like HZ 43, the spectrum in the 100-200 eV region would resemble that of a 300,000 black body, for the temperatures in the vicinity of 10^5 K which we derive. Correction for interstellar absorption indicates that $[L_x/L_v]_o$, its value at the surface of H1504, is 11 ± 4. (This uncertainty includes the uncertainty in the zero point caused by uncertainties in what parameters to use for HZ 43.) This would fit a pure H model at T(eff) = 98,000 K. Adding very substantial quantities of trace He, with N(He) = 0.01, characteristic of the DO stars, would increase the derived temperature to 150,000 K.

The He-rich models of Wesemael (1981), near T(eff) = 150,000 K, resemble 400,000 K black bodies, and so the correction for interstellar absorption is a bit less than in the H-rich case, with $[L_x/L_v]_o$ = 9.6 $\pm$ 4. There is some modest gravity sensitivity to the value of $[L_x/L_v]$ determined from the models, and so the derived temperature using He-rich models is 156,000 K for log g = 8, with an estimated uncertainty of 10,000 K produced by an uncertainty in log g. The grid of models is rather sparse; with $[L_x/L_v]$ increasing by a factor of 2 when one decreases log g from 8 to 7 at 200,000 K, and with a change in the other direction at 100,000 K.

The black body analysis proceeds along similar lines, where one used Nugent et al.'s Fig. 4 to estimate corrections for interstellar H (which vary with the blackbody temperature), and one compares a

efficiency changes dramatically. For example, the soft X-ray flux inferred from a given count rate changes by a factor of twenty when the assumed incident spectrum is changed from a 100,000 K black body to a 200,000 K black body. Hence we can not infer a temperature or even a flux in the soft X-ray band without knowledge from other data of the incident spectral shape.

To escape this extreme model dependency we have chosen to form a completely empirical quantity, $[L_x/L_v]$, based on the ratio of X-ray to optical flux between H1504 and HZ 43. We define

$$[L_x/L_v] = \frac{[f_x/f_v]_{H1504+65}}{[f_x/f_v]_{HZ43}} ,$$

where the f's are the observed fluxes. To first order the ratio f_x/f_v takes out differences in distance and stellar radius, so $[L_x/L_v]$ should be one, if H1504 and HZ 43 have the same spectrum (HZ 43 was selected as a reference because it was well observed optically and by HEAO-1 and EXOSAT). $[L_x/L_v]$ is found to be 8.1 $\pm$ 2, indicating that H1504 has a spectrum proportionately emitting more X-rays than HZ 43.

To achieve quantitative temperature estimates it is necessary to invoke models, but by making the comparisons in terms of $[L_x/L_v]$ we hope that model inadequacies will also cancel to first order. We used a 60,000 K pure hydrogen model to represent the spectrum of HZ 43. Uncertainties in the temperature or spectrum of HZ 43 affect this scheme, but by a small amount; a 3000 K change in the temperature of HZ 43 changes the value of $[L_x/L_v]$ by only 1.5, a small effect in light of the tremendous leverage offered by observations of thermal X-rays.

An additional correction to be made is that for interstellar absorption. Nugent et al. (1983) in Fig. 4, give corrections which

black body spectrum to the HZ 43 spectrum and calculates $[L_x/L_v]_o$.
Since the black body spectrum is considerably softer than the spectra
of H or He models at similar temperatures, the correction for inter-
stellar absorption absorption is greater. The best fit is for T =
$(166 \pm 10) \times 10^3$ K.

e) Attempts to Model the EXOSAT Count Rates

The EXOSAT observations of H1504+65 consist of count rates ob-
tained from three overlapping, but significantly different broad band
filters covering the wavelength range 100-240 $\overset{o}{A}$. At the very lowest
energies the response in the EXOSAT filter bands is a more senitive
measure than the HEAO-1 proportional counter. Potentially then, we can
constrain the effective temperature of H1504+65 in terms of published
models. The approach is as follows. As we remain largely ignorant of
the true atmosphere composition of H1504+65 we investigate four quite
different types of model atmospheres; a simple black body, pure H
models (Wesemael et al. 1980), pure He models (Wesemael 1981), and
solar composition models characteristic of the central stars of
planetary nebulae (Hummer and Mihalas 1970). For each model (except
black body), we employ gravities in the range log g = 7.5 to 8.0 and
normalize to the observed visual magnitude (V = 16.24). EXOSAT count
rates are then computed as a function of temperature and interstellar
column density, N_H. For each filter the observed count rate and its
associated statistical uncertainly correspond to a band of temperatures
and N_H in the $T_{eff} = N_H$ plane. Acceptable models correspond to
regions where the three filter defined bands mutually overlap.

No one model, or set of models, simultaneously predicts the
observed EXOSAT count rates in all three EXOSAT filters. More over,

very few models succeed in predicting observed count rates for reasonable values of N_H ($< 10^{20.5}$ cm^{-2}). In general the disagreements are very large. Expressed in terms of the 1σ error bars in the count rates given in sec. IVb the discrepancies are at the 10-20 σ level. Inconsistencies of this magnitude greatly exceed those which might be attributed to our knowledge of the effective areas used to define the filter band passes. Clearly we have not correctly modeled the soft X-ray flux from H1504+65. This is perhaps not unexpected since none of the models considered should be expected to provide an adequate representation of soft X-ray fluxes from H1504+65. A black body is of course a poor approximation in the soft X-ray (Shipman 1976). The pure H models completely lack important He II and metal opacities and are consequently too bright. He rich models, which might apply to PG 1159 objects, too thoroughly quench the soft X-ray flux, and produce almost no flux below the He II ionization edge at 227 Å (which is where virtually all the EXOSAT counts are observed.) At exceedingly high temperatures (T >> 150,000) He rich models may begin to provide sufficient flux, but the predicted ratio of EXOSAT filter rates is inconsistent with the data. At intermediate He content the unblanketed, LTE, solar composition models of Hummer and Mihalas also produce mutually inconsistent EXOSAT count rates. This particular situation is illustrated in Figure 7 where effective temperatures and interstellar column densities corresponding to the observed count rates in the three EXOSAT filters are shown.

It is clear that until representative model atmospheres become available soft X-ray fluxes from such objects will remain difficult to interpret. To illustrate, the EXOSAT count rates for H1504+65 are

black body spectrum to the HZ 43 spectrum and calculates $[L_x/L_v]_o$. Since the black body spectrum is considerably softer than the spectra of H or He models at similar temperatures, the correction for interstellar absorption absorption is greater. The best fit is for T = $(166 \pm 10) \times 10^3$ K.

e) Attempts to Model the EXOSAT Count Rates

The EXOSAT observations of H1504+65 consist of count rates obtained from three overlapping, but significantly different broad band filters covering the wavelength range 100-240 Å. At the very lowest energies the response in the EXOSAT filter bands is a more senitive measure than the HEAO-1 proportional counter. Potentially then, we can constrain the effective temperature of H1504+65 in terms of published models. The approach is as follows. As we remain largely ignorant of the true atmosphere composition of H1504+65 we investigate four quite different types of model atmospheres; a simple black body, pure H models (Wesemael et al. 1980), pure He models (Wesemael 1981), and solar composition models characteristic of the central stars of planetary nebulae (Hummer and Mihalas 1970). For each model (except black body), we employ gravities in the range log g = 7.5 to 8.0 and normalize to the observed visual magnitude (V = 16.24). EXOSAT count rates are then computed as a function of temperature and interstellar column density, N_H. For each filter the observed count rate and its associated statistical uncertainly correspond to a band of temperatures and N_H in the $T_{eff} = N_H$ plane. Acceptable models correspond to regions where the three filter defined bands mutually overlap.

No one model, or set of models, simultaneously predicts the observed EXOSAT count rates in all three EXOSAT filters. More over,

contrasted in Table 1 with those of two recognized PG 1159 objects, PG 1159-035 and K1-16, and with the DA white dwarf HZ 43. The last column of Table 1 gives a soft X-ray to optical luminosity ratio, normalized to 1.0 for PG 1159-035, for all four objects. Note that PG 1159-035 and K1-16 have similar luminosity ratios while H1504+65 is considerably larger.

VI. DISCUSSION

   a) What is H1504+65?

   There is considerable data for this star, but the above sections
indicate that it does not seem easy to fit it with existing models. We
can conclude that it is definitely not a DA white dwarf star, a hot
analog of HZ 43. The implied X-ray temperatures are far too cool to be
consistent with the absence of Balmer lines. Even a model with sub-
stantial trace He, with T(eff) = 150,000 K, produces an Hγ line with a
strength, depending on gravity, of 1.2 - 2 A, incompatible with the
optical spectrum. The disagreement between model and data is
sufficiently great that we believe we can rule out this explanation.

   Our attempts to fit the Wesemael pure He models to this object
also did not succeed, but the discrepancies between model and observa-
tion are not as drastic. The X-ray data suggest a temperature of
160,000 K. Wesemael does not provide any calculations of He line
strengths for temperatures higher than 150,000 K (see his Figure 7).
The models indicate that the He lines are weakening with increasing
temperature, but that they are still quite strong at 150,000 K (1.26 A
for log g = 6 and 3.23 A for log g = 8). Additional modeling would be
required to decide, definitively, whether the He lines fall off fast
enough with increasing T(eff) so that a He-dominated atmosphere with
a T(eff) of around 160,000 K would be consistent with an upper limit
to the strength of this line of 0.5 A. Additional problems with
the He interpretation are the steepness of the ultraviolet continuum
and the failure to fit the various EXOSAT data points.

   If the primary constituent of the atmosphere is neither H nor He,
what could it be? The only spectral features that we see are C IV and

contrasted in Table 1 with those of two recognized PG 1159 objects, PG 1159-035 and K1-16, and with the DA white dwarf HZ 43. The last column of Table 1 gives a soft X-ray to optical luminosity ratio, normalized to 1.0 for PG 1159-035, for all four objects. Note that PG 1159-035 and K1-16 have similar luminosity ratios while H1504+65 is considerably larger.

O VI. While any definitive investigation of the possibility that we are seeing a carbon-oxygen dominated atmosphere must await further modeling, some qualitative and semi-quantitative considerations indicate that this suggestion is reasonably consistent with the features that we observe. At this high temperautre, with an electron density of 10^{17} (characteristic of optical depth unity), C is mostly C V, with some C IV at shallower depths. C V, a He-like ion, is essentially unobservable; its ionization potential is very high, 391 eV, and the resonance lines are in the X-ray part of the spectrum. The only possible problem with the C spectrum that we observe is whether the weak C IV lines that are seen in the optical spectrum are consistent with the IUE data, which shows the C IV resonance lines to be marginal at best. In a high-density, high-temperature atmosphere, O will exist as O V, O VI, and O VIII. Except for the O VI resonance doublet at 1031 and 1037 A, which we have detected, these species all have their resonance lines in the EUV spectral region, where we couldn't see them. Whether the features that we detect (O VI 1032, 1038, and 3434) are consistent with absence of the O VI lines at 3811 and 3834 A remains to be seen. Perhaps the 3811 and 3834 A lines are heavily broadened, or even shifted to become the unidentified features seen at 3860 and 3885A.

To summarize, the line spectrum that we see suggests a C-O dominated atmosphere, with no obvious resonance lines missing, although the absence of C IV 1548, 1550 and O VI 3811, 3834 is perhaps puzzling. Without detailed models, we are not prepared to claim that we have discovered a white dwarf star of this unique, if not unexpected, composition. Such modeling is clearly a high priority task for the immediate future, as is the calculation of models with the composition and

$T_{eff} > 150,000$ K. It is nevertheless true that, unlike the cooler hot degenerates like HZ 43 and the DO stars, existing models are unable to account for many pieces of information: the different X-ray count rates from EXOSAT, the ultraviolet continuum slope, and the absence of H I and He II lines, although it is possible that a He-dominated model could be generated which would produce the necessary temperature and the absence of He II.

So far, very little has been said about surface gravity, except for some comparisons with the PG 1159 objects which indicate that H1504+65 has a surface gravity comparable to that of PG 1159 (log g = 7). There are, however, independent arguments, based on its faintness and position in the sky, which constrain it to be a degenerate or near degenerate. The optical flux from a stellar photosphere is relatively independent of composition, varying by about 30% from H- to He-dominated models. The fundamental relationship between monochromatic Eddington flux H_ν, the flux received at earth f_ν, the stellar radius R, and its distance D is (Shipman 1979)

$$f_\gamma = 4\pi \, H_\nu (R/D)^2$$

With H1504+65 at a galactic latitude of 46°, one can use plausibility arguments to constrain acceptable values of R. A temperature of 160,000 K determines the value of H_ν in eq. 1. From the observed value of f_ν, we have relationship between R and z: $(R/0.03\,R_\Theta) = (z/850\text{ pc})$. $(R = 0.03\,R_\Theta$ corresponds to log g = 7, for a plausible mass of 0.6 solar masses.) 850 pc is already implausibly large as a distance from the galactic plane; gravities less than log g = 7 are probably excluded simply because of this object's faintness and its position in the sky. We conclude that H1504+65 is a degenerate or

O VI. While any definitive investigation of the possibility that we are seeing a carbon-oxygen dominated atmosphere must await further modeling, some qualitative and semi-quantitative considerations indicate that this suggestion is reasonably consistent with the features that we observe. At this high temperautre, with an electron density of 10^{17} (characteristic of optical depth unity), C is mostly C V, with some C IV at shallower depths. C V, a He-like ion, is essentially unobservable; its ionization potential is very high, 391 eV, and the resonance lines are in the X-ray part of the spectrum. The only possible problem with the C spectrum that we observe is whether the weak C IV lines that are seen in the optical spectrum are consistent with the IUE data, which shows the C IV resonance lines to be marginal at best. In a high-density, high-temperature atmosphere, O will exist as O V, O VI, and O VIII. Except for the O VI resonance doublet at 1031 and 1037 A, which we have detected, these species all have their resonance lines in the EUV spectral region, where we couldn't see them. Whether the features that we detect (O VI 1032, 1038, and 3434) are consistent with absence of the O VI lines at 3811 and 3834 A remains to be seen. Perhaps the 3811 and 3834 A lines are heavily broadened, or even shifted to become the unidentified features seen at 3860 and 3885A.

To summarize, the line spectrum that we see suggests a C-O dominated atmosphere, with no obvious resonance lines missing, although the absence of C IV 1548, 1550 and O VI 3811, 3834 is perhaps puzzling. Without detailed models, we are not prepared to claim that we have discovered a white dwarf star of this unique, if not unexpected, composition. Such modeling is clearly a high priority task for the immediate future, as is the calculation of models with the composition and

near-degenerate, with a temperature of $(160 \pm 30) \times 10^3$ K, and log g greater than 7. Our error estimate is greater than that suggested by any of the individual model fits, and is a rather subjective one which allows for the absence of any model to fit the data.

b) Evolutionary Considerations

Cautiously accepting our temperature of 160,000 K, and our limit that $7 < \log g < 8$, we can place H1504+65 in the HR diagram, as shown in Fig. 10. The evolutionary tracks are from Kawaler, Hansen, and Winget (1985). The evolutionary time scales associated with these objects are quite short, as was dramatically confirmed when the pulsation period change in PG 1159-035 was observed by Winget et al. (1985). Depending on the mass of H1504, the time that it would take to cool to the temperature of PG 1159-035 is only of the order of 10^5 yr. Since $[L_x/L_v]$ of H1504 is 600 times the corresponding value for PG 1159, this change in X-ray brightness is about 0.2 percent per year or 2 percent in a decade. These strictly empirical considerations suggest that such a change might be observable with a sufficiently long-lived spacecraft, especially considering that one could make a differential measurement in comparison with a constant X-ray source with a similar spectrum such as HZ 43.

It is also apparent from Figure 2 that H1504+65 is in the part of the H-R diagram occupied by the hotter planetary nebula nuclei (PNNs), as are the PG 1159 objects. The PNN of the nebula K1-16 also exhibits pulsations similar to PG 1159-035 (Grauer and Bond 1984). Many of the PNNs showing strong O VI and C IV emission features are believed to have very high temperatures and He/CNO-enriched surfaces. Since at least most white dwarfs are believed to be descended from planetary

nebulae, one may ask where is the nebula around H1504+65 (and likewise the isolated PG 1159 objects)? One possible answer is the occurrence of a late helium shell flash, resulting in the ejection of the remaining residual hydrogen, the exposure of helium and/or CNO-rich material at the surface, and the return of the PNN to the region of the Harmon-Seaton sequence after the original hydrogen-rich nebula has dissipated (Iben et al. 1983). Such a scenario may be developed to explain any highly unusual surface abundances in H1504+65 in particular.

A third evolutionary consideration is the clear difference in temperature between objects like H1504+65 and PG 1159-035 entering the white dwarf stage and the hottest of the more numerous DA white dwarfs with hydrogen-rich surfaces. One decade after HZ 43 and Feige 24 were discovered as EUV sources, it has been difficult to establish any DA white dwarfs which are substantially hotter than these well-analyzed stars near 50,000-60,000 K. While $\sim$ 100,000 K DA stars would be expected to show up as strong soft X-ray sources, none were found in the X-ray surveys (Nugent et al. 1983). Fleming, Liebert and Green (1985) find no DA star hotter than about 80,000 K among the complete sample of over 300 white dwarfs (and several hundred more subdwarf O and B stars) in the PG Survey. Yet six PG 1159 stars near 100,000 K and log g $\sim$ 7 with helium-rich atmospheres, were found from the same sample, and H1504+65 appears in this sample as well.

The hottest stars entering the white dwarf sequence with hydrogen-rich compositions include the DAO stars with traces of helium (such as HZ 34; Wesemael et al. 1985) and a few PNNs (such as Abell 7 near 75,000 K and log g $\sim$ 7 and NGC 7293 near 90,000 K and log g $\sim$ 6.6; Mendez, Kudritzki and Simon 1983). The differences in temperature (at

near-degenerate, with a temperature of $(160 \pm 30) \times 10^3$ K, and log g greater than 7. Our error estimate is greater than that suggested by any of the individual model fits, and is a rather subjective one which allows for the absence of any model to fit the data.

b) Evolutionary Considerations

Cautiously accepting our temperature of 160,000 K, and our limit that $7 < \log g < 8$, we can place H1504+65 in the HR diagram, as shown in Fig. 10. The evolutionary tracks are from Kawaler, Hansen, and Winget (1985). The evolutionary time scales associated with these objects are quite short, as was dramatically confirmed when the pulsation period change in PG 1159-035 was observed by Winget et al. (1985). Depending on the mass of H1504, the time that it would take to cool to the temperature of PG 1159-035 is only of the order of 10^5 yr. Since $[L_x/L_v]$ of H1504 is 600 times the corresponding value for PG 1159, this change in X-ray brightness is about 0.2 percent per year or 2 percent in a decade. These strictly empirical considerations suggest that such a change might be observable with a sufficiently long-lived spacecraft, especially considering that one could make a differential measurement in comparison with a constant X-ray source with a similar spectrum such as HZ 43.

It is also apparent from Figure 2 that H1504+65 is in the part of the H-R diagram occupied by the hotter planetary nebula nuclei (PNNs), as are the PG 1159 objects. The PNN of the nebula K1-16 also exhibits pulsations similar to PG 1159-035 (Grauer and Bond 1984). Many of the PNNs showing strong O VI and C IV emission features are believed to have very high temperatures and He/CNO-enriched surfaces. Since at least most white dwarfs are believed to be descended from planetary

a given luminosity) between stars approaching their final white dwarf radii with hydrogen-rich and hydrogen-poor envelopes may be explainable in terms of stellar evolution models, if the former have hydrogen layers with masses of order 10^{-4} of the stellar mass (Iben and Tutukov 1984, see also Koester and Schönberner 1985).

Table 1

H1504+65 Compared to Other EXOSAT Observed Hot Stars

	V	3000 Å Lexan[a]	Aℓ + Paralene[a]	Lx/Lv[b]
HZ 43[c]	12.86	28	21	110
PG1159-035	14.84	0.041[d]	<0.0015[d]	1.00
K1-16	15.09	0.0233[d]	0.0032[d]	0.72
H1504+65	16.24	6.97	0.017	617

a) counts/sec.

b) X-ray (3000 Å Lexan) to optical ratio (PG1159-035 = 1)

c) Heise 1984

d) Holberg, private communication

a given luminosity) between stars approaching their final white dwarf radii with hydrogen-rich and hydrogen-poor envelopes may be explainable in terms of stellar evolution models, if the former have hydrogen layers with masses of order 10^{-4} of the stellar mass (Iben and Tutukov 1984, see also Koester and Schönberner 1985).

We gratefully acknowledge the assistance of many capable scientists in such a multiplr instrument, broad wavelength coverage observational effort. D. Weedman and A. Wasilewski searched and collected the objective prism plate. L. Takalo helped with the BMO observations and data reduction. F. Marshall halped with the Palomar observations. T. Fleming assisted in the analysis of the 2.3 m and MMT spectroscopic data. IUE data analysis was performed at the Goddard Regional Data Analysis Facility. H. Giclas provided the limit to the proper motion of H1504+65. The EXOSAT Telescope Observing team provided the HZ 43 data in advance of publication. J. Heise provided useful discussions of the observations of white dwarfs with EXOSAT. E. Sion provided helpful comments on an earlier draft of the manuscript.

REFERENCES

Auer, L. and Shipman, H. 1977, Ap.J. Letters 211, L103.

Boggess, A. et al. 1978, Nature 275, 372.

Broadfoot et al. 1977, Space Sci. Rev., 21, 183.

Broadfoot et al. 1981, J. Geophys. Res., 86, 8259.

de Jager, C. 1980, The Brightest Stars, (Dordrecht: Reidel), ch. 3.

de Korte, P.A.J. et al. 1981, Sp. Sci. Reviews 30, 495.

Drilling, J.S., Holberg, J.B. and Schönberner, D., 1984, Ap.J. (Letters),
    283, L67.

Fleming, T., Liebert, J. and Green, R.F. 1985, Ap.J. in press.

Giclas, H. 1985, private communication.

Grauer, A.D. and Bond, H.E. 1984, Ap.J., 277, 211.

Heiles, C. 1975, Astr. and Ap. Suppl. 20, 37.

Heise, J. 1984, 18th ESLAB Symposium, "X-ray Astronomy", The Hague.

Holberg, J.B., Forrester, W.T., Shemansky, D.E. and Barry, D.C. 1982,
    Ap.J., 257, 656.

Holberg, J., Wesemael, F. and Hubeny, I. 1984, Ap.J. 280, 697.

Hummer, D.G. and Mihalas, D. 1970, MNRAS 147, 339.

Iben, I. and Tutukov, A.V. 1984, Ap.J., 282, 615.

Iben, I. andTutukov, A.V. 1985, in press.

Iben, I., Kaler, J.B., Truran, J.W. and Renzini, A., Ap.J., 264, 605.

Kahn, S., Wesemael, F., Liebert, J., Raymond, J., Steiner, J., and
    Shipman, H. 1984, Ap.J. 278, 255.

Kawaler, S.D., Hansen, C.J. and Winget, D.E. 1985, Ap.J. 295, 547.

Koester, D., and Schönberner, D. 1985, Ast. Ap. in press.

Malina, R.E., Bowyer, S., and Basri, G. 1982, Ap.J. 262, 717.

Martin, C., Basri, G., Lampton, M., and Kahn, S. 1982, Ap.J. Letters

261, L81.

Mendez, R., Kudritzki, R. and Simon, K. 1983, on Planetary Nebulae,
Proc. of IAU Symp. No. 103, ed. D.R. Flower, D. Riedel Press,
Dordrecht, p. 343.

Morton, D.C. 1967, Ap.J. Letters 156, L97.

Nugent, J.J. et al. 1983, Ap.J. Suppl. 51, 1.

Paresce, F. 1984, A.J. 89, 1022.

Ramsey, L.W., Nations, H.L., and Barden, S.C. 1981, Ap.J. Letters
251, L101.

Rothschild, R. et al. 1979, Sp. Sci. Instrum. 4, 9.

Shipman, H.L. 1976, Ap.J. Letters 206, L67.

Sion, E.M., Liebert, J. and Starrfield, S.G. 1985, Ap.J. 292, 471.

Wesemael, F., Auer, L.H., Van Horn, H.M., and Savedoff, M.P. 1980,
Ap.J. Suppl. 43, 159.

Wesemael, F., Green, R., and Liebert, J. 1985, Ap.J. Suppl. 58, 379.

Wesemael, F. 1981, Ap.J. Suppl. 45, 177.

Winget, D.E., Kepler, S.O., Robinson, E.L., Nather, R.E. and O'Donoghue,
D. 1985, Ap.J. 292, 606.

FIGURE CAPTIONS

Figure 1 — Finding chart for H1504+65 (α, δ = $15^h01^m23^s.1$, +66°24'09"). From the Palomar Sky Survey E Plate.

Figure 2 — Combined spectra of H1504+65.

Figure 3a — Multiple Mirror Telescope blue-sensitive Reticon scan of the 4050 to 4950 Å region of H1504+65. The sharp emission line due to C IV λ4686 and He II λ4658 is indicated. Upper limits for Hγ, Hβ, He II λ4686 and He II λ4540 correspond to equivalent widths of $\sim$ 0.5 Å.

Figure 3b — A 2.3 m Steward optical ultraviolet Reticon scan of the 3200 to 4300 Å region of H1504+65. The presence of a broad, centrally reversed, O VI feature at λ3434.7 and possible weaker features due to the same ion at 3314 and 3622 Å are indicated. Also shown is a broad shallow depression corresponding to the C IV feature present in other PG 1159 objects. (Sion, Liebert and Starrfield, 1985).

Figure 4 — Low resolution short wavelength ultraviolet spectrum of H1504+65. Sum of 4 SWP exposures by IUE. Lyman alpha portion of spectrum is taken from small aperture spectrum showing interstellar absorption with equivalent width of 5.7 $\pm$ 1 Å.

Figure 5 — Low resolution long wavelength ultraviolet spectrum of H1504+65. Sum of one LWR and two LWP exposures by IUE.

Figure 6 — The ultraviolet spectral indices, defined over the 1250-1800 A range, as a function of stellar temperature. Circles: Wesemael (1981) pure He models. Squares: Wesemael pure H models. Crosses: the black body relation. Observed points from PG 1159 and H1504 are shown.

Figure 7 — Regions of T_e - N_H model space consistent with EXOSAT
filter observations for Hummer and Mihalas (1970) planetary nebula
central star models.

Figure 8 — The HR diagram. Error bars show the position of H1504+65
(this paper) and the PG 1159 objects (Holberg et al. 1985). The
evolutionary tracks are from Kawaler et al. Numbers in boxes are
the ages, where the zero point is set by assigning an age of 3000
yr at log L = 3.0, in thousands of years. The large hatched
region is the region occupied by the nuclei of planetary nebulae
according to Pottasch (Planetary Nebulae, 1984, fig IX-1).

ADDRESSES OF AUTHORS

Paolo Giommi and N.E. White, ESOC, Robert Bosch Strasse 5, 6100

   Darmstadt, West Germany.

J.B. Holberg, Lunar and Planetary Laboratory, University of Arizona,

   3625 East Ajo Way, Tucson, AZ 85713.

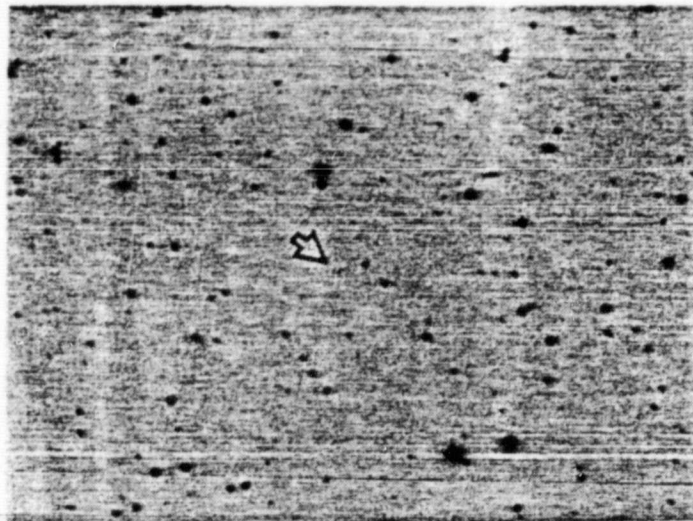James Liebert, Steward Observatory, University of Arizona, Tucson,

   AZ 85726.

J.A. Nousek, Department of Astronomy, 525 Davey Lab., The Pennsylvania

   State University, University Park, PA 16802.
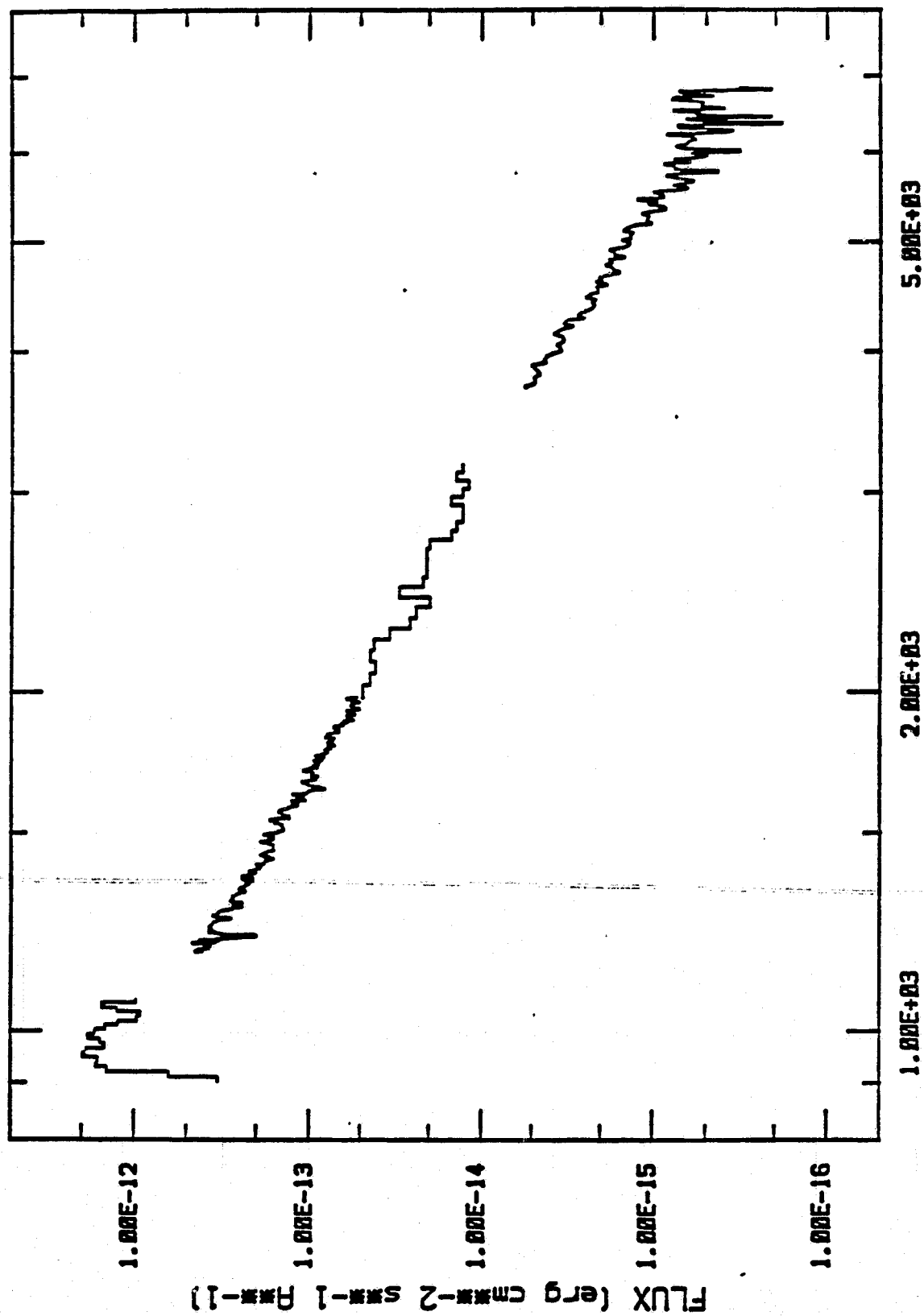
Steven H. Pravdo, Jet Propulsion Laboratory, M.S. 183-701, 4800 Oak

   Grove Drive., Pasadena, CA 91109.

Harry L. Shipman, Physics Department, University of Delaware, Sharp

   Lab., Newark, DE 19716.

NE

ADDRESSES OF AUTHORS

Paolo Giommi and N.E. White, ESOC, Robert Bosch Strasse 5, 6100
Darmstadt, West Germany.

J.B. Holberg, Lunar and Planetary Laboratory, University of Arizona,
3625 East Ajo Way, Tucson, AZ 85713.

James Liebert, Steward Observatory, University of Arizona, Tucson,
AZ 85726.

J.A. Nousek, Department of Astronomy, 525 Davey Lab., The Pennsylvania
State University, University Park, PA 16802.

Steven H. Pravdo, Jet Propulsion Laboratory, M.S. 183-701, 4800 Oak
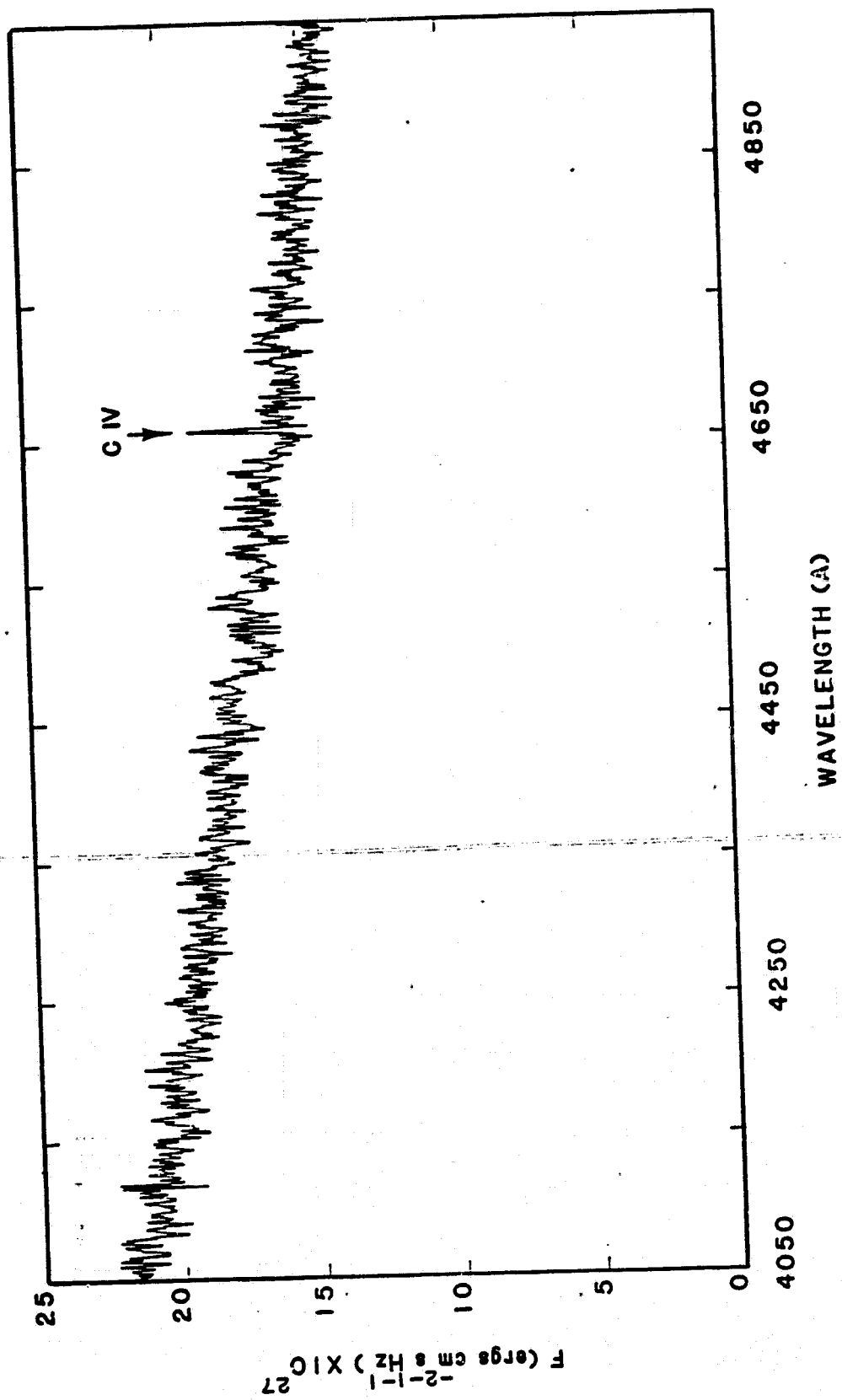Grove Drive., Pasadena, CA 91109.

Harry L. Shipman, Physics Department, University of Delaware, Sharp
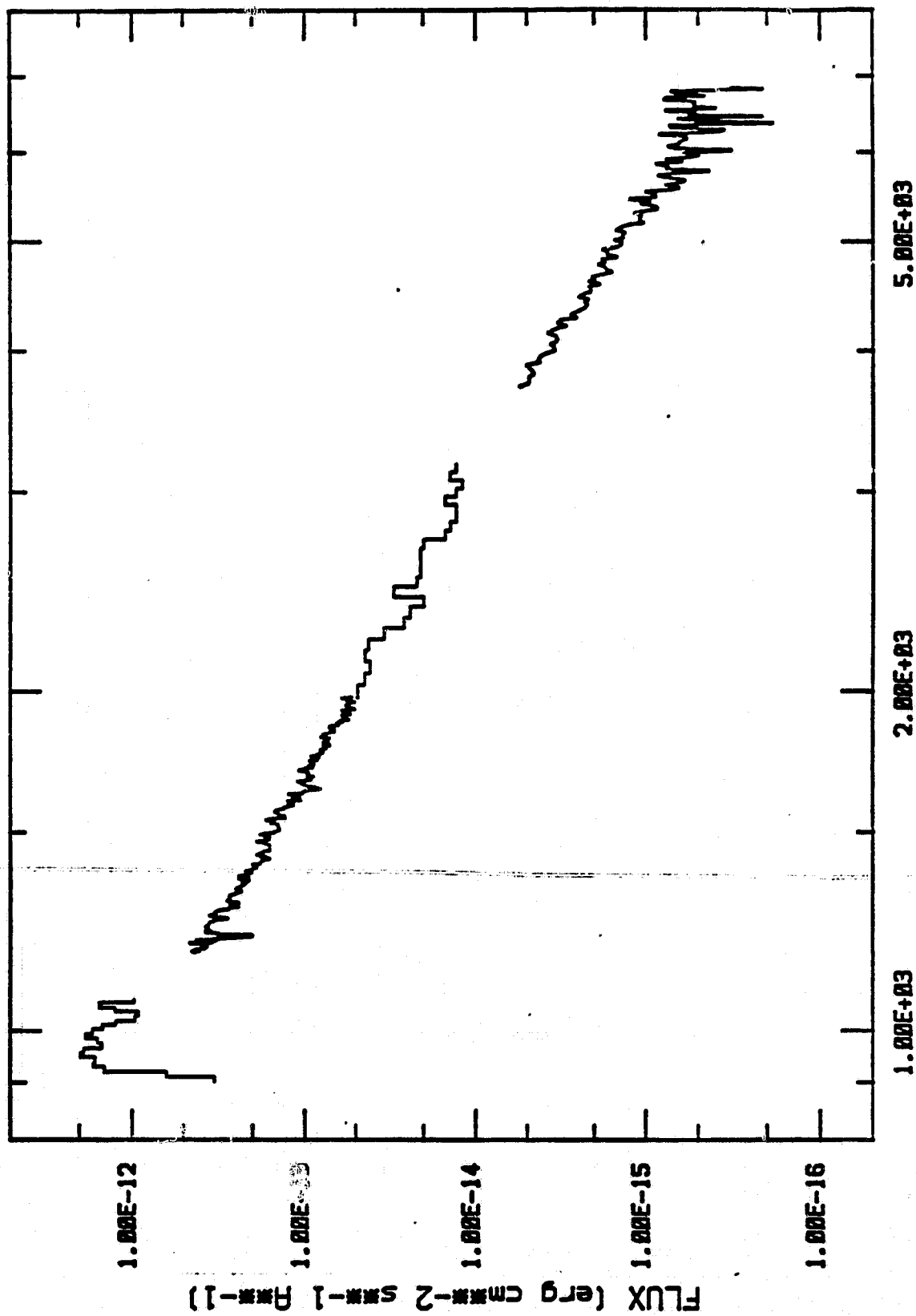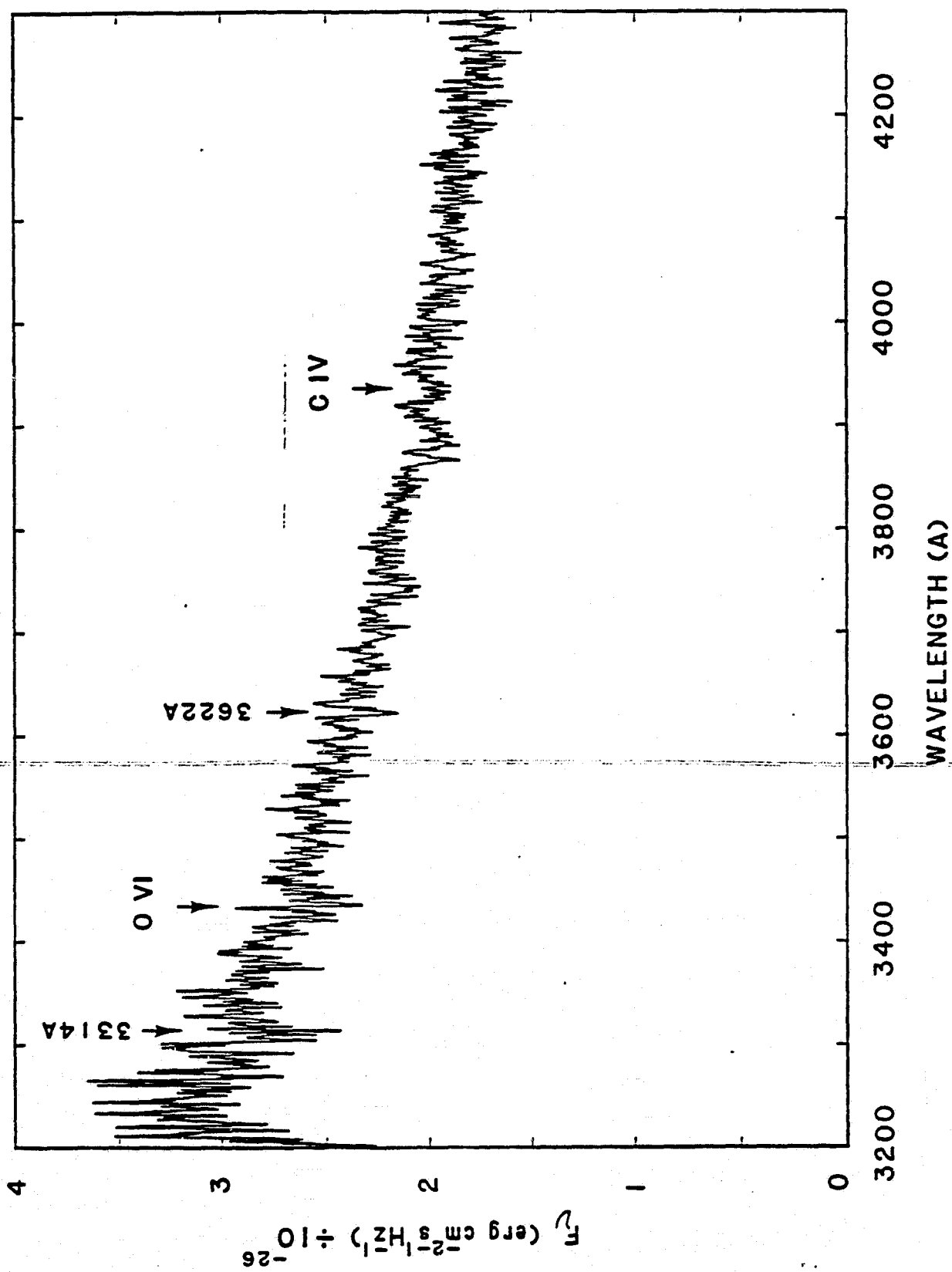Lab., Newark, DE 19716.

COMBINED SPECTRUM OF H1504+65

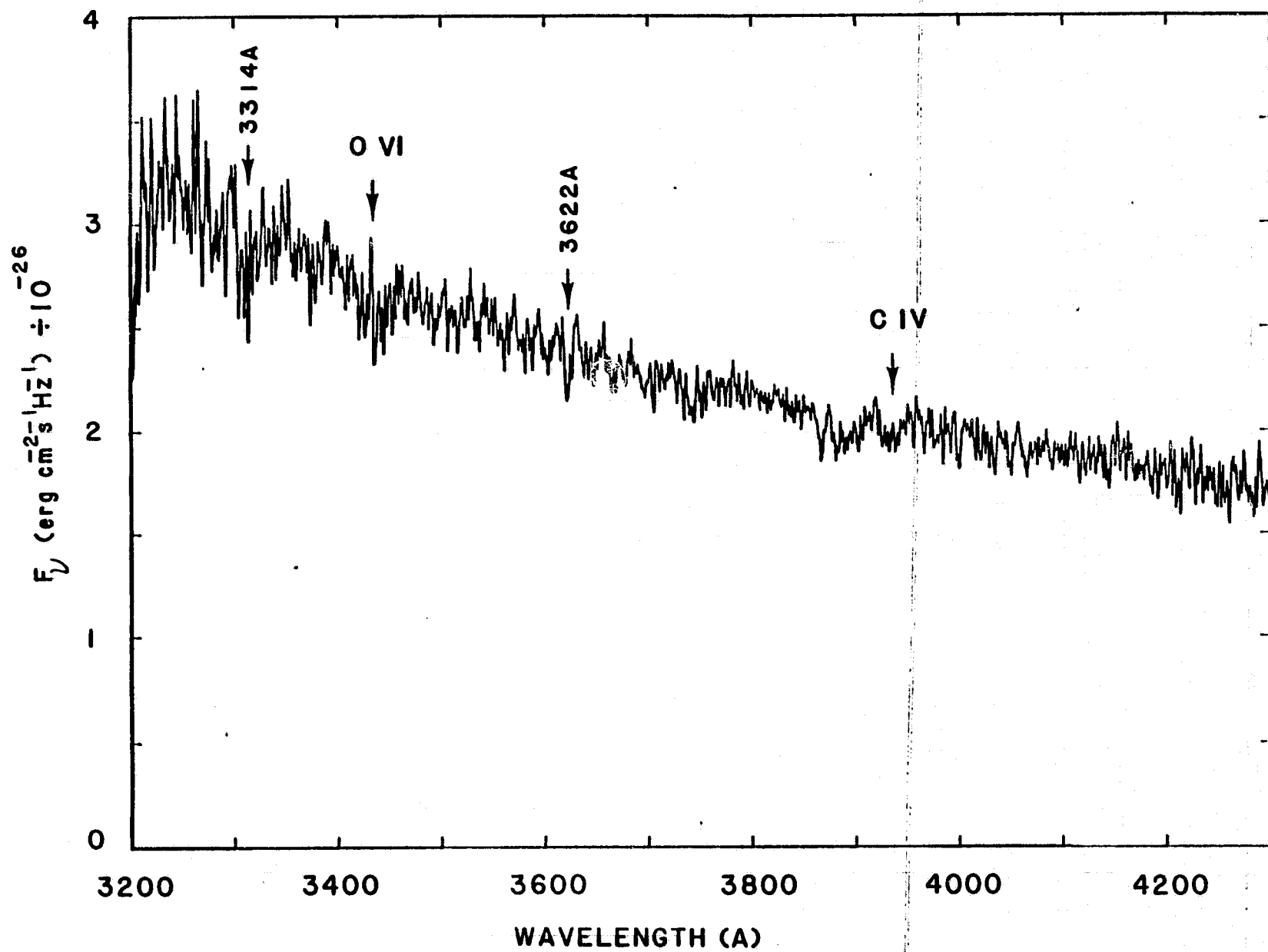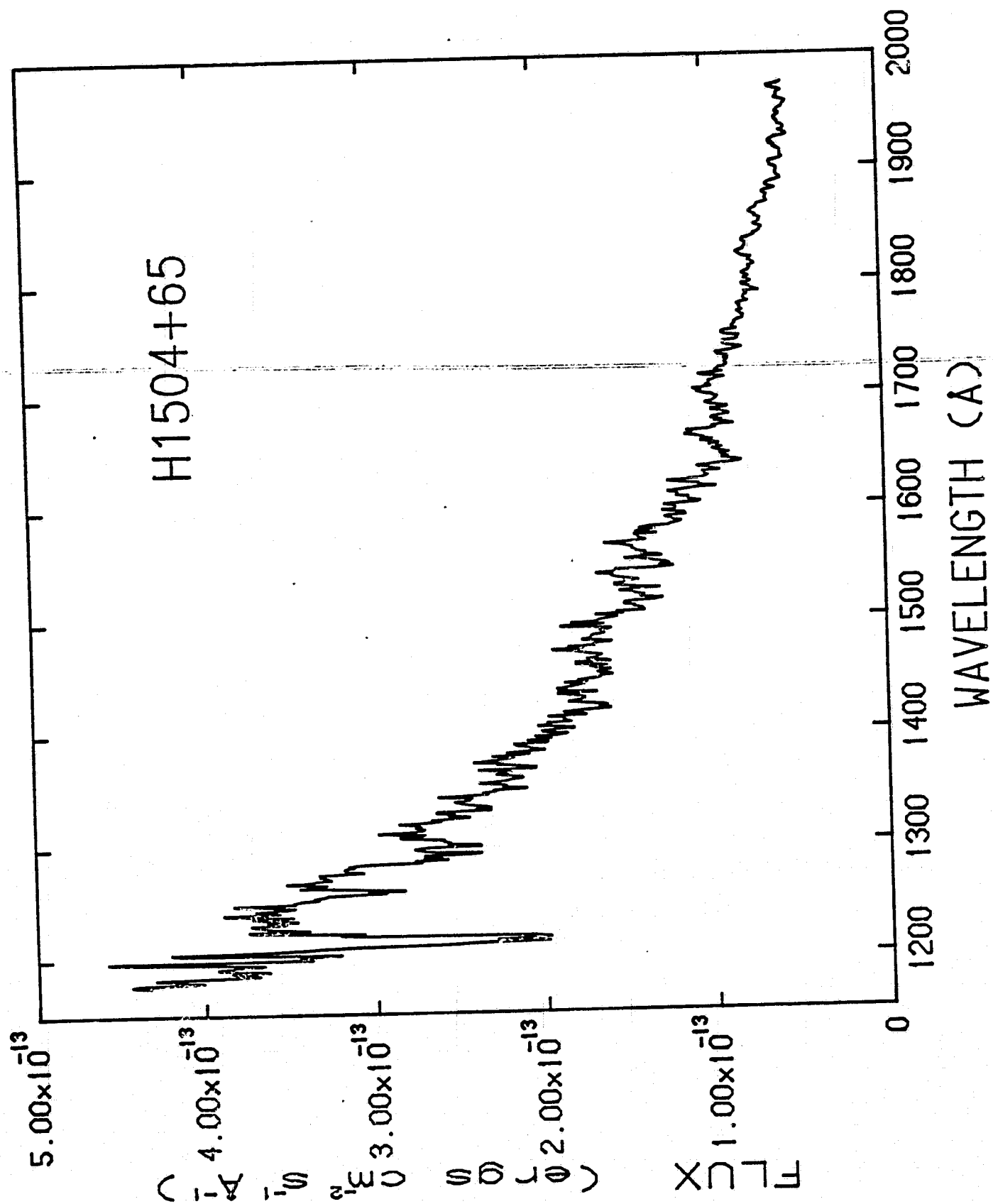Y-axis: F (ergs cm^{-2} s^{-1} Hz^{-1}) X10^{27}

X-axis: WAVELENGTH (Å)

C IV

COMBINED SPECTRUM OF H1504+65

WAVELENGTH (ANGSTROMS)

FLUX (erg cm**-2 s**-1 A**-1)

CIV

3622A

O VI

3314A

WAVELENGTH (Å)

F_ν (erg cm^{-2}s^{-1}Hz^{-1}) $\div 10^{-26}$

4200 4000 3800 3600 3400 3200

4 3 2 1 0

H1504+65

FLUX (ergs cm^{-2} s^{-1} Å^{-1})

WAVELENGTH (Å)

H1504+65

Figure showing log N_H (cm^{-2}) versus $T_{eff}/10^3$ (K) with curves labeled Boron, Al/P, and 3000Å Lexan.
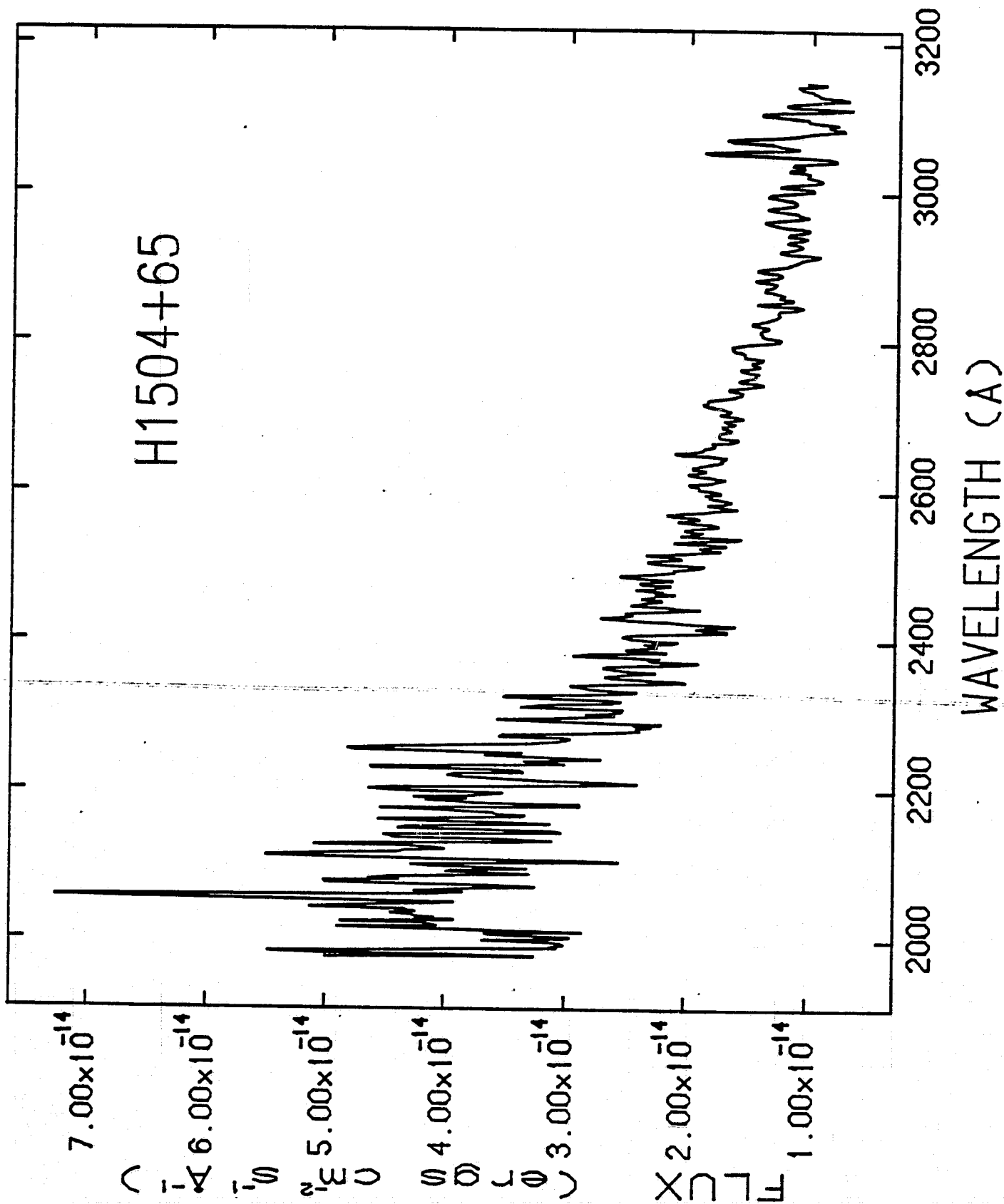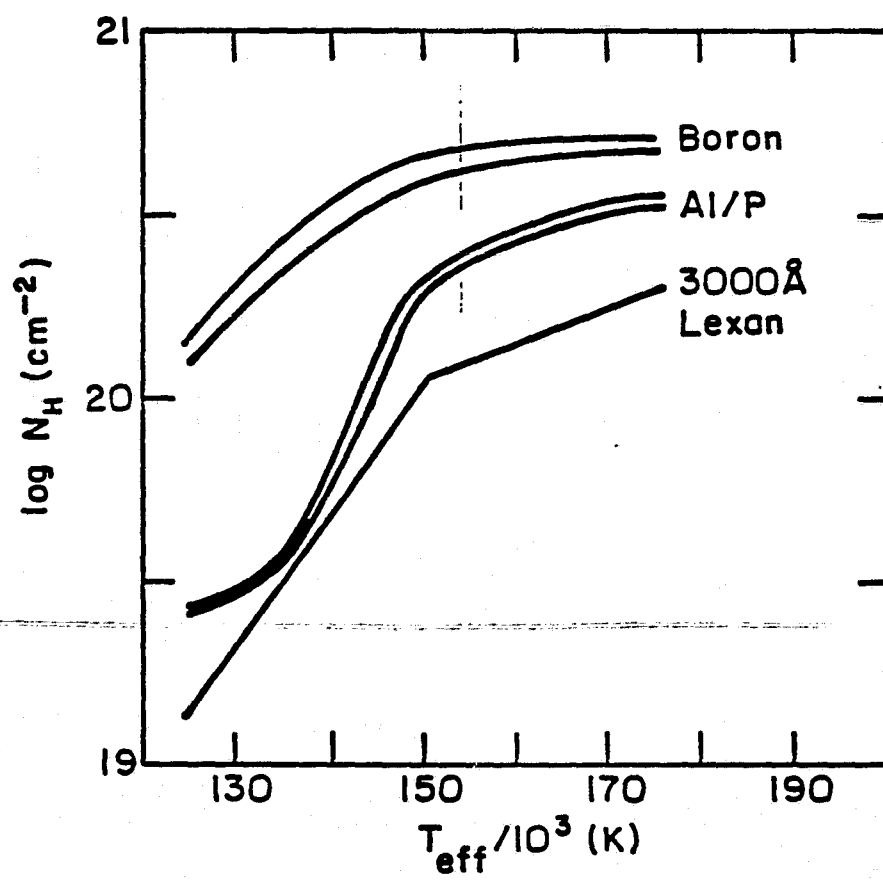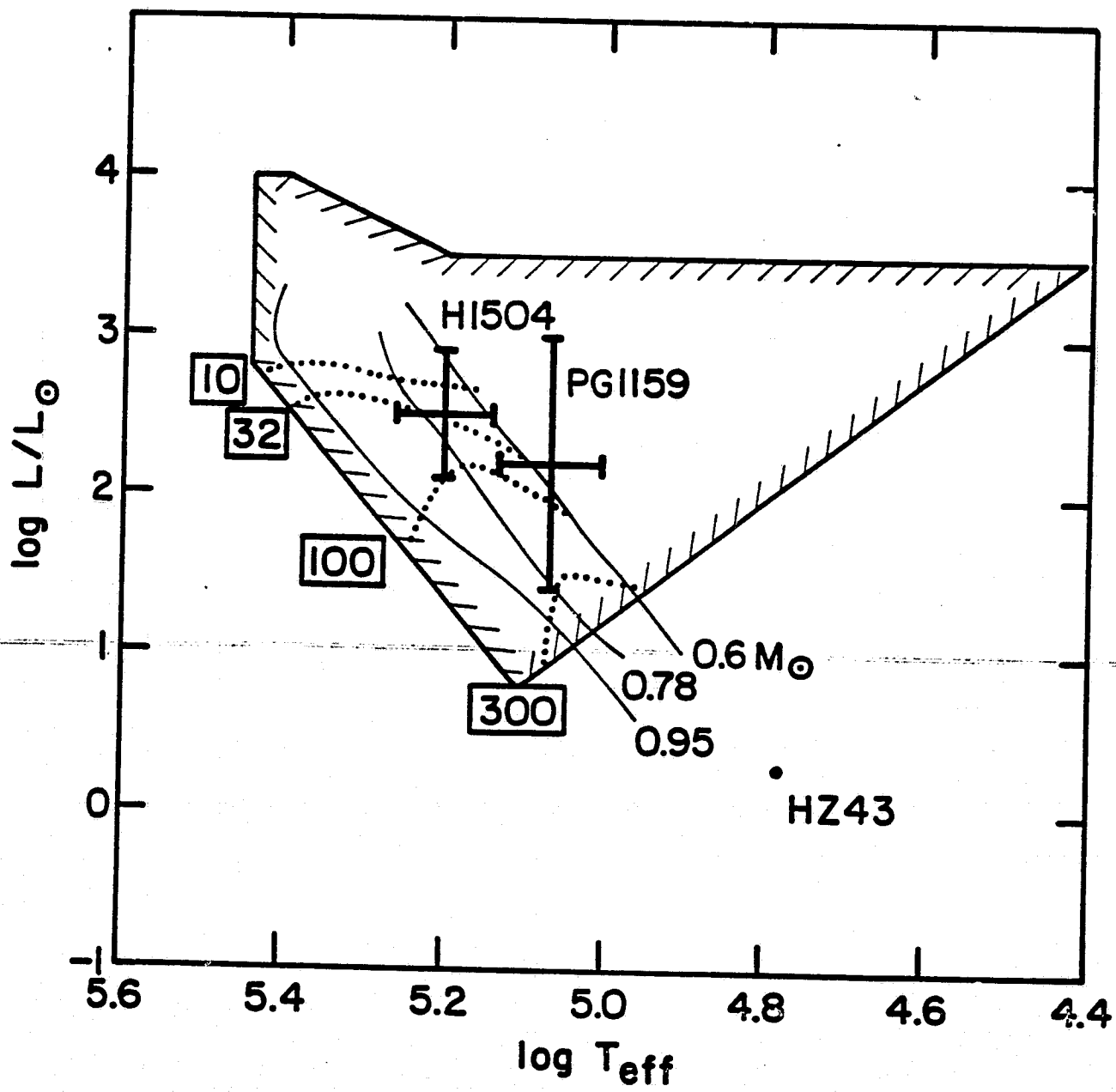
Temperature, radius and rotational velocity of Sirius B.

by Peter Thejll and Harry L. Shipman.
Physics Department, University of Delaware,
Newark, Delaware 19716.

Abstract.

Based on the theoretical work, by Ostriker and Hartwick (1968), concerning the magnetic fields of rotating white dwarfs, and the recent determination of the effective temperature, by Holberg et al. (1984), we have derived the interrelationships between radius, rotational velocity and effective temperature for Sirius B.

We find that i) the radii, 0.76 to 0.81 in hundredths of solar radii, predicted by T_{eff} between 26000 and 28000K and a mass of $1.05M_o$ places Sirius B somewhat above the Hamada-Salpeter mass-radius relation, by about 1 or 2 σ. ii) the rotational velocity of Sirius B is predicted to lie between 0 and 600 km/s (using 2 σ limits) and that only radii which place a white dwarf above the mass-radius line are allowed. iii) in order to further limit the rotational velocity and the radius of Sirius B better determinations of T_{eff} and magnitude are needed. If the satellite HIPPARCOS can determine the parallax of Sirius B with 1 milliarcsecond accuracy then the errors on T_{eff} and the magnitude will be the limiting factors in the future.

Keywords: Sirius B - rotating white dwarfs - magnetic fields - Mass/Radius relation.

I. Introduction.

The motivation for our work is twofold. We want to check if Sirius B falls on the mass-radius (M-R) relation using new data from Holberg et al. (1984). Only a few objects have so far been placed conclusively on that relation. We also wish to present a new method for determining rotational velocities for cases when the standard method, of modeling rotationally broadened lines, doesn't work.

Many determinations of Sirius B's properties have been made over the years. Greenstein, Oke and Shipman (1971) analyzed the H_α and H_γ line profiles and arrived at T_{eff} = 32000 +/- 1000K, along with gravity and radius: R/R_o = 0.0078 +/- 0.0002. Shipman (1976) pointed out that a pure Hydrogen model with T_{eff} = 32000K would have the low absorption coefficient in the X-ray region necessary to explain the X-ray observations by Mewe et al. (1975). This value of T_{eff} was obtained using unblanketed model atmospheres. If blanketed atmospheres had been used, this value of T_{eff} would have been lowered by 2000K. Later determinations of T_{eff} have confirmed the general conclusion that Sirius B is much hotter than Sirius A, but also lowered the T_{eff} somewhat. Bohm-Vitense, Dettman and Kapranidis (1979) found T_{eff} = 26000 +/- 1000K by fitting theoretical models to IUE spectra of Sirius B. Later Martin, Basri and Lampton (1982) used HEAO1 A-2 data and fitted a 28000K model finding support for a photospheric origin of the X- rays. Using the IUE data and UV data from Voyager 2 Holberg, Wesemael and Hubeny find support for T_{eff} in the range 26000 - 28000K with a firm upper limit at 28000K. EXOSAT data will also provide a constraint on the T_{eff}, although

uncertanties in the EXOSAT calibration are still being investigated.

One open question is whether, given all these determinations of T_{eff}, Sirius B fits on the M-R relation. One reason Sirius B might not fit the mass- radius relation is that rotation can increase its radius (Ostriker and Hartwick, 1968). While one can analyze the rotationally broadened line profiles (Pilachowski and Milkey, 1984) this method is only applicable to stellar spectra with very high resolution - and thus only useful for a few bright stars. Another possibility is that residual nuclear burning could increase the radius from its zero temperature value, as has been shown by Koester and Schonberner (1986) for 0.6 M_o stars. A similar calculation for the $1M_o$ case has not been done, but the effects of nuclear burning would be smaller, and possibly negligible, for a higher mass.

Ostriker and Hartwick established the relationship between radius, magnetic field and angular momentum for a white dwarf of mass $1.05M_o$. We can use their work to get the relationships between radius, rotational velocity and temperature, provided that we have an upper limit to the magnetic field strength and have values for orbital elements, the magnitude and the parallax. We have applied this method to Sirius B.

II. Method.

From Keplers third law one can calculate the total mass of the Sirius system and use the accurately known *fractional* mass of Sirius B to find its mass. The radius of Sirius B is found by using the calculated relationship between absolute flux and effective temperature (Shipman 1979, table 2) and the magnitude and parallax (Gatewood and Gatewood, 1978). In using the Ostriker and Hartwick (1968) results we assume that Sirius B rotates as a homogeneous sphere and that there is essentially no magnetic field on Sirius B. We base this last assumption on inspections of high-resolution spectra of the H_α and H_γ lines (Greenstein, Oke and Shipman, 1971, unpublished spectra).

As we used Ostriker and Hartwicks results we found that the $v_{eq}=0$ line fell above the Hamada-Salpeter mass-radius relation. We assume this is because Ostriker and Hartwick did not sufficiently model the envelope of white dwarfs and that if they had done so the $v_{eq}=0$ line would have fallen on the Hamada Salpeter M-R relation. Thus we *put* $v_{eq}=0$ on the M-R line for a C^{12} body. We assumed the angular momentum of Sirius B could be modeled by using the moment of inertia of a homogeneous sphere. Using a more realistic mass distribution ($\rho(r)r^2 = const.$) makes only a 20% difference in the equatorial rotational velocity v_{eq}.

In fig.1. we plot the results of our analysis in a M-R diagram. We have drawn lines parallel to the Hamada-Salpeter relation through each point determined by velocity and mass - we are thus assuming that the M-R lines for non-zero velocities will look like this in a small area close to the HS line. Fig.2 is a more detailed nomogram where the relationships between T_{eff}, radius and rotational velocities can be seen for a $1.05M_o$, homogeneous, spherical white dwarf.

III. Uncertainties.

The quantities that enter our calculations are of course in error to some extent - to see how important these errors are we both calculated the propagation of errors and introduced 1σ shifts in the parallax and the magnitude to see the effects. (See fig. 1.) The sizes of the relative errors σ_{rel} on the quantities that determine the mass of Sirius B are:

$$(\sigma_{rel}(M_B))^2 = (3\sigma_{rel}(\pi))^2 + (3\sigma_{rel}(\alpha))^2 + (\sigma_{rel}(f_B))^2 + (2\sigma_{rel}(P))^2$$

or

$$(0.0261)^2 = (0.0246)^2 + (0.0079)^2 + (0.0030)^2 + (0.0022)^2$$

where π, α, f_B and P are; parallax, angular semi-major axis of the orbit, the fractional mass of Sirius B and the period of the orbit. The 3% error is mainly due to the error on the parallax, α contributes about one tenth as much.

The error on the radius, determined from $H(T_{eff})$, π and magnitude m, is dominated by the error on the magnitude:

$$(\sigma_{rel}(R_B))^2 = (\ln 10/5 \; m \; \sigma_{rel}(m))^2 + (\sigma_{rel}(\pi))^2 + (\sigma_{rel}(H(T_{eff})/2))^2$$

or

$$(0.0192)^2 = (0.0166)^2 + (0.0082)^2 + (0.005)^2$$

where we have assumed that the relative error on $H(T_{eff})$ is 1% - a reasonable number, as will be discussed in section IV. The error on the magnitude contributes about four times as much as does the error on the parallax. We have used an absolute error on the magnitude of $(0.03)^2 + (0.02)^2$ where the last term takes into consideration the absolute calibration error. It is obvious that an improved determination of the magnitude is called for. Perhaps it is impossible, at the present epoch of the Sirius B orbit, and with standard techniques, to improve significantly on the value for the magnitude, but, as Smith and Terrile (1984) point out in their paper on the β Pictoris disk the sort of equipment they used is very well suited for photometric work near bright sources, such as the Sirius system.

How will the capabilities of the HIPPARCOS satellite change matters? If it can determine parallaxes to within 1 milliarcsecond then the error on M_B that π introduces will be the same as that from the semi-major axis and furthermore the uncertainty on the magnitude will overshadow that on the parallax by a factor of nearly 40 in its influence on the relative error of R_B.

IV. Discussion of the methods.

We determine the radius R of Sirius B by using the fundamental relation between the stellar flux f, the monochromatic Eddington flux at the stellar surface $H(T_{eff})$, and the stellar distance D, from Shipman 1979:

(1) $\quad R = D \ (f/(4\pi H(T_{eff})))^{1/2}$

Because of the sensitivity of the results we discuss to relatively small uncertainties in the values of various input quantities, we include a considerable discussion of the above equation and the uncertainties therein, and ask for the readers' patience with what is in places a pedagogical discussion. Earlier discussions of errors have been given by Shipman (1979) and, with respect to the accuracy of the $H(T_{eff})$ relation, by Wesemael et al. (1980).

An advantage of this method, and of all surface brightness methods for determining a stellar radius, is that you do not need to know (or guess) how much energy the star is emitting at all wavelengths. The disadvantage is that you must be able to determine the stellar flux H accurately. But this problem can be circumvented or minimized by carefully choosing the wavelength or wavelength range over which you fit the above equation to the data. Provided that you apply the equation at a wavelength which is shortward of the Planck maximum, the dependence of H on T_{eff} is relatively weak - linear in the black-body approximation - which minimizes the uncertainty in R produced by uncertainties in T_{eff}.

In this paper we apply it in the V band, since the V flux from Sirius B is known to within 0.03 magnitudes. In contrast, Bohm-Vitense et al. applied the equation in the IUE spectral range, which one might think to be superior, being closer to the Planck maximum at these temperatures. However, model calculations indicate otherwise. $H_{5405 \ A}$ increases by 33% when you increase T_{eff} from 30,000K to 35,000 K, while $H_{1363 \ A}$ increases by 57% (Shipman, unpublished, blanketed, non-LTE models; the Wesemael et al. models are virtually identical, as is shown in table 1). Thus, a 1,000 K uncertainty in T_{eff} produces an uncertainty of 6.6% in H (and 3.3% in R) when you use this method in the V band, and an uncertainty of 11% in H (5.5% in R) when you use the method in the IUE spectral range. This consideration, by itself, suggests that the visual band is the one to work with.

The ultraviolet spectral band is not as useful for application of equation (1), although it is essential if one is to determine T_{eff} accurately. The correction for scattered light in the IUE spectral range is considerable, being smallest at the shortest wavelengths, and is uncertain, since one has to use an existing spectroscopic instrument rather than a specially constructed area scanning photometer. In addition, the uncertainty in the overall IUE absolute calibration is usually quoted at 10% (see, e.g., R.C. Bohlin, et al., 1980 and R.C. Bohlin, 1985). Individual readers can make their own judgments of the accuracy of the IUE measurements of the Sirius B UV flux, but it is at least as uncertain as

the overall calibration uncertainty of 10%. Our examination of the figures in Bohm-Vitense et al. suggests that the uncertainty in measuring f generated by the need for correcting for scattered light is probably half of the total correction, or, at the shortest wavelengths, about 15%, producing an overall error in f of $(10)^2 + (15)^2$ or 18%, which corresponds to 9% in R arising from uncertainties in the flux measurements alone, if you apply equation (1) in the IUE spectral range.

An additional consideration which must be applied in an investigation of this kind is how good are the models; how well can you trust the $H(T_{eff})$ relation which enters equation (1) ? This point has been discussed earlier by, e.g., Auer and Shipman (1977), Shipman (1979b) , and most extensively by Wesemael et al. (1980). The ATLAS program, used for the $H(T_{eff})$ relation used here (and in Shipman 1979), and the Auer-Mihalas program as modified by Wesemael, used for the Wesemael et al. calculations, are completely independent. The uncertainties in $H_{5405 A}$ for a given T_{eff} are really quite small (see table 2.); at $T_{eff} = 20,000$ K, comparing blanketed models with blanketed models, the relative change in H_{5405} calulated as $(H_{Shipman} - H_{Wesemael}/H_{Shipman})$ is +0.0059, at $T_{eff} = 30,000$ K it is -0.0032 and it is -0.0061 at $T_{eff} = 50,000$ K. Using unpublished, non- LTE models calculated at Delaware indicates a realtive change in $H_{5405 A}$ calculated as $(H_{nonLTE} - H_{LTE})/H_{LTE} = 0.011$ at 35,000 K. This scale is quite gravity independent; going from log(g) of 8 to 8.5 at 30,000 K decreases the Eddington flux, in these same relative terms, by -0.0082. The uncertainties in the $H(T_{eff})$ relation are thus far smaller than that of the magnitude and can safely be estimated at about 1% or less.

V. Results.

On fig. 1 one sees that the temperature range that Holberg et al. arrived at corresponds to a range in radii of from 0.76 to 0.81 in 100R/R$_o$. This is above the C^{12} mass-radius relation of Hamada and Salpeter, but if 1σ shifts are introduced in magnitude, mass and parallax then Sirius B moves onto the M/R relation. Not until the errors on magnitude, parallax and of course T_{eff} are reduced, as discussed above, can the issue of Sirius B's placement on or off the mass-radius relation be settled.

From the Holberg et al. temperatures and the Ostriker and Hartwick results we find the velocity to lie between 0 and 600 km/s - these are the velocity limits that a 2σ circle, centered at (M,R), touches. Furthermore, only positive rotational velocities are allowed, so only the part of the M-R plane above the C^{12} line is accessible. Any temperature and mass determinations that place Sirius B, or any other white dwarf, below the line can thus be ruled out.

VI. Discussion.

Some interesting considerations, and some suggestions for current work, emerge from a consideration of how the astrometric data on Sirius are likely to improve in the future. The European satellite HIPPARCOS can improve the parallax of Sirius significantly; the current best parallax (Gatewood and Gatewood, 1978) has an uncertainty of 3 milliarcseconds, and the advertised HIPPARCOS capability should improve this by a factor of 3. Such improvement can, in principle allow us to determine the radius with much greater precision than we can now. In addition, at the present time the uncertainty

in the mass is dominated by the uncertainty in the parallax; with a perfect parallax, the uncertainty in the relative orbit produces a mass with an uncertainty of 0.9% (compared with the current value of 2.5%), where the uncertainty in the relative orbit contributes equally to the total uncertainty in the mass.

At that time this analysis can be done with considerable more precision, if our estimates of the temperature, and of the visual magnitude, or the absolute flux at any wavelength, of Sirius B, can be improved significantly over the present values. At the moment, the uncertainty in parallax, temperature, and visual magnitude all contribute roughly equally to the uncertainty in the radius; in the future, the magnitude and temperature will dominate. This suggests that continued efforts to improve the accuracy of particularly the visual magnitude and of the temperature of the companion will be worthwhile.

$T_{eff}\backslash\lambda$	5405 A	1363 A
30,000 K	3.41e-4	1:98e-3
35,000 K	4.545e-4	3.116e-3
[H(35)-H(30)]/H(30)	0.333	0.574
ΔT=1000 K	ΔH=0.067	ΔH=0.115
	ΔR=0.033	ΔR=0.057

Table 1: Showing the sensitivity of $H(T_{eff})$ to changes in T_{eff} in the V band and the IUE spectral range. The sensitivity is least in the V band. From unpublished models by Shipman.

T_{eff}	HS	Wesemael et al.	HS $\log(g)=8.5$
20,000 K	1.70e-4	1.69e-4	(+0.005)
30,000 K	3.41e-4	3.421e-4	(-0.0082)
50,000 K	6.49e-4	6.58e-4	(+0.013)

Table 2: Showing $H_{5405 \, A}$, as calculated by Shipman and Wesemael et al. using completely different programs, for different T_{eff} and $\log(g)$. The first two coloumns are for $\log(g)=8$ and the last is for the change in H when going from a $\log(g)=8$ to a $\log(g)=8.5$ model, relative to the $\log(g)=8$ model. Note the very small dependencies of H on $\log(g)$ and choice of program. Modified from Table 1 of Wesemael et al. 1980.
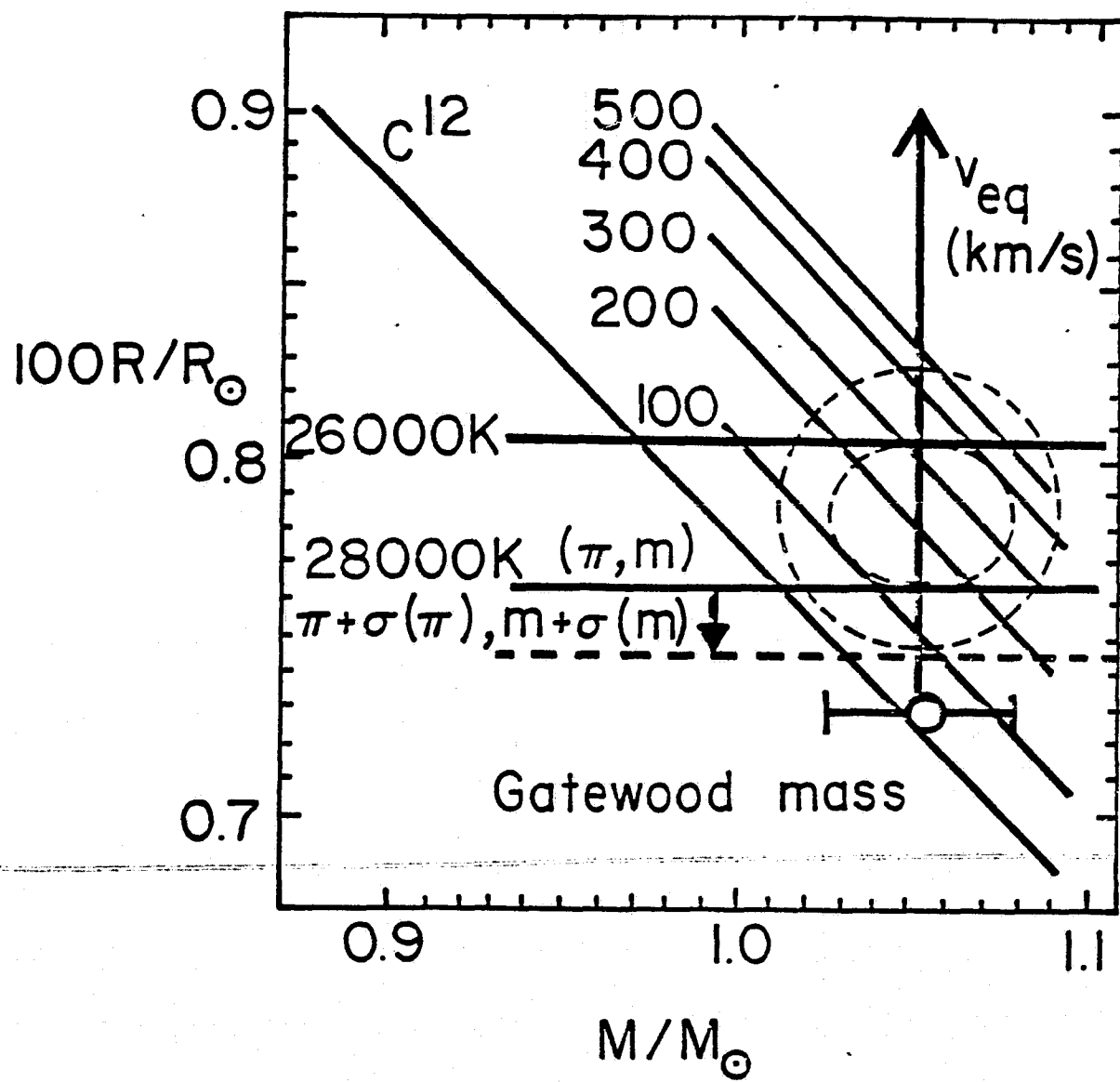
Fig.1. Mass-Radius diagram for a 1.05 M_0 white dwarf, like Sirius B. The line marked C^{12} is the Hamada-Salpeter zero temperature mass-radius relation and the two horizontal lines represent the radii calculated from the upper and lower limits on T_{eff} set by Holberg et al. Astrometric data and the magnitude was taken from Gatewood and Gatewood. If 1 sigma shifts are introduced in the magnitude and the parallax the radius-line given by 28000K moves down to the dashed line, showing the influence of errors on the input data. The velocity scale gives the equatorial rotational velocity in km/s for a homogenous, spherical body, modified from data given by Hartwick and Ostriker. The two circles have radii 1 and 2 sigma, respectively.
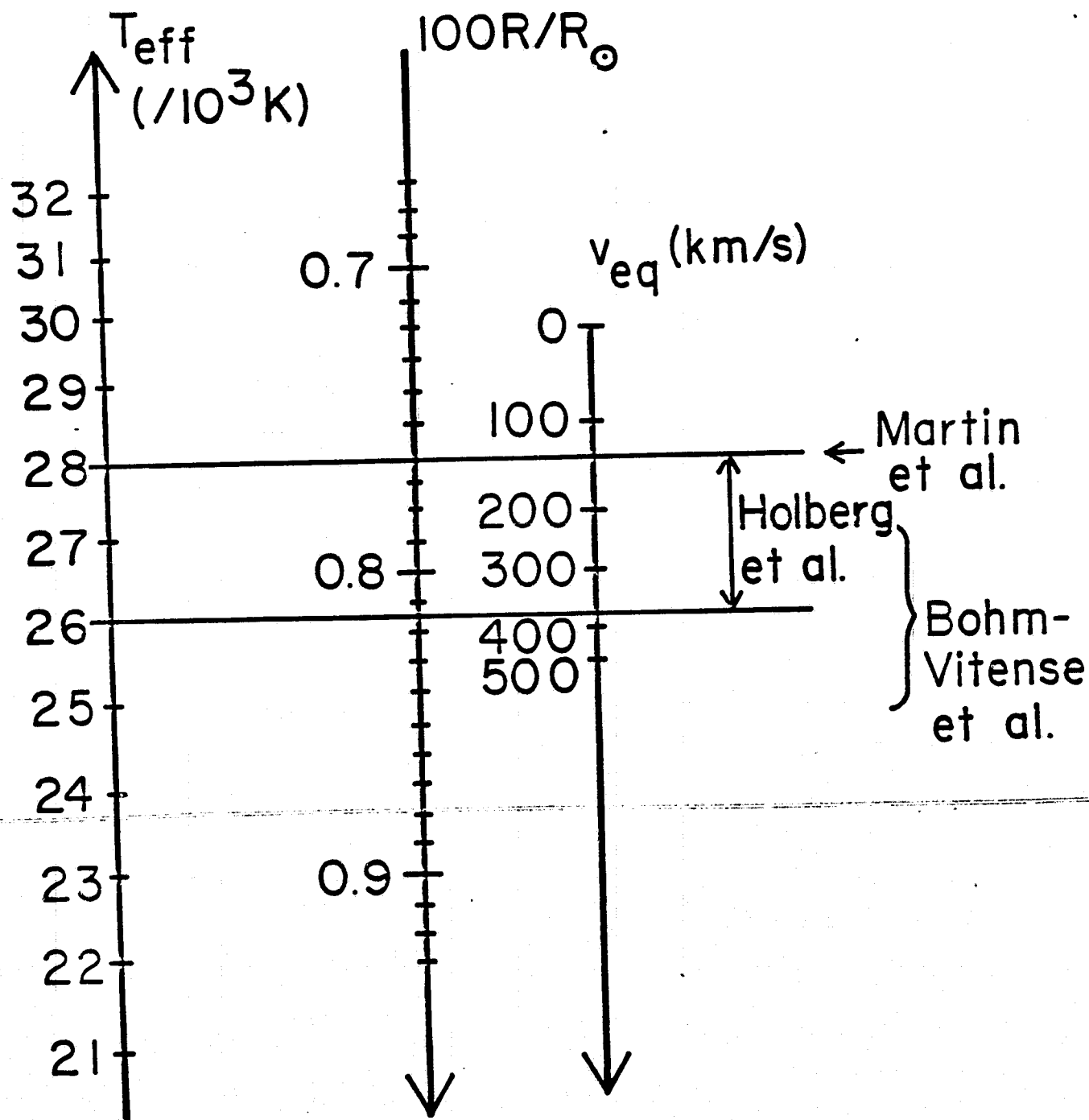
Fig.2. Nomogram showing how T_{eff}, radius and equatorial rotational velocity relate for a 1.05 M_0 white dwarf like Sirius B. The calculations assume a spherical homogenous mass distribution and use data from Hartwick and Ostriker, Gatewood and Gatewood and unpublished spectra of Sirius B from Greenstein, Oke and Shipman.

References.

Auer, L, H, and Shipman, H.L., 1977, *Ap. J. Lett.* 211, L103.

Bohlin, R.C., et al., 1980, *Astron. Astrophys,* 85, 1.

Bohlin, R.C., 1985, *NASA IUE Newsletter,* No. 26, 20.

Bohm-Vitense, E., Dettman, T. and Kapranidis, S. 1979, *Ap. J. Lett.,* 232, L189.

Gatewood, G.D., Gatewood, C.V., 1978, *Ap. J.,* 225, 191.

Greenstein, J.L., Oke, J.B. and Shipman, H.L., 1971, *Ap. J.,* 169, 563.

Holberg, J.B., Wesemael, F. and Hubeny, I., 1984, *Ap. J.,* 280. 679.

Koester, D. and Schonberner, D., 1986, *Astron. Astrophys,* 154, 125.

Martin, C., Basri, G. and Lampton, M., 1982, *Ap. J. Lett.,* 261. L81.

Mewe, R., et al., 1975, *Nature,* 256. 711.

Milkey, R.W. and Pilachowski, C.A., 1984, *PASP.,* 96, 821.

Ostriker, J.P. and Hartwick, F.D.A., 1968, *Ap. J.* 153. 797.

Rakos, K. D. and Havlen, R.J. 1977, *Astron. Astrophys.,* 61, 185.

Shipman, H.L., 1976, *Ap. J. Lett.,* 206, L67.

Shipman, H.L., 1979, *Ap. J.,* 228. 240.

Shipman, H.L., 1979b, *IAU Colloquium,* No. 53. 86.

Smith, B.A. and Terrile, R.J., 1984, *Science.* 225, 1421.

Wesemael, F., et al., 1980, *Ap. J. Supp. Ser.* 43. 159.

EXOSAT OBSERVATIONS of V471 TAURI :
I. A 9.25 MINUTE PULSATION from the WHITE DWARF and ORBITAL PHASE DEPENDENT X-RAY ABSORPTION DIPS

K.A.Jensen
 Naval Research Laboratory
 Goddard Space Flight Center

J.H.Swank, R.Petre
 Goddard Space Flight Center

E.F.Guinan, E.M.Sion
 Villanova University

H.L.Shipman
 University of Delaware

ABSTRACT

A 28 hour continuous EXOSAT observation of the 0.52 day period detached binary V471 Tauri has detected a strong, pulsed soft X-ray flux from the white dwarf component, with a 9.25 minute pulse period, an amplitude of ~20%, and a double peaked pulse profile. A residual soft X-ray flux from the K dwarf companion is seen during white dwarf eclipse at orbital phase 0.0. Pronounced dips in the soft X-ray light curve occur at orbital phases 0.15, 0.18, and 0.85. The dips may be correlated with the ~~outer~~ *triangular* Lagrangian points of the binary orbit. Smaller dips at phases near the eclipse may be associated with cool loops in the K star corona at heights of 0.2 stellar radii. The X-ray flux from the white dwarf is consistent with thermal models for a white dwarf photosphere with $T_{eff} \sim 35000$ K, log g = 8.0-8.5, log N[He/H] < -4.5, and log N_H = 18.65 +/- 0.2. The K star has a luminosity of 1.5 +/- 0.3 x 10^{30} ergs s^{-1} in the 0.03-2.5 keV band.

I. INTRODUCTION

V471 Tauri (BD+16°516) is a well known 0.52 day binary containing a hot DA white dwarf and a K2V detached companion. As a member of the Hyades cluster (Young and Capps 1971) it has a presumed age of 5×10^8 years and a distance of 49 +/- 1 pc (Vandenberg and Bridges 1984). Young and Nelson (1972) derived a sini = 1.1×10^{11} cm, $\overline{\sin}$ i = 79°.5 +/- 2°.0, $M_K = 0.8\ M_\odot$, $M_W = 0.8\ M_\odot$, $R_W = 6.5 \times 10^8$ cm. The white dwarf mass and radius are accurate to within 15%, and are consistent with the Hamada-Salpeter (1961) mass-radius relation for white dwarfs with log g = 8.2-8.5. Model atmosphere fits to IUE low dispersion spectra have determined $T_{eff} \approx 35000$ K and log g ~ 8.0 (Guinan and Sion 1984). The absence of He II, C IV, and Si IV lines in the IUE spectra at a sensitivity of 0.5 Å equivalent width constrain the photospheric helium abundance to be log N[He/H] < -3.0 and constrain the carbon and silicon abundances to be less than 10^{-1} solar. (cf. Henry, Shipman, and Wesemael 1985). The K dwarf's synchronous rotation is one of the most rapid known for a nondegenerate star in a detached system. (Wall Ref?)

Van Buren, Charles, and Mason (1980) identified V471 Tau as a HEAO A-2 LED X-ray source. They considered the K star corona to be the likely X-ray source, but did not rule out accretion of a K star wind onto the white dwarf. V471 Tau was detected as an Einstein Observatory IPC source by Young et al. (1983), who also considered the K star to be the probable X-ray

source, although their observations did not cover white dwarf eclipse phases.

In this Letter we report new results obtained from a 28 hour continuous observation of V471 Tauri with the European Space Agency EXOSAT satellite : the detection of soft X-ray fluxes from both the white dwarf and the K dwarf, the discovery of a 9.25 minute pulsation from the white dwarf, and the discovery of orbital phase related soft X-ray dips.

II. OBSERVATIONS

The EXOSAT X-ray satellite was pointed at V471 Tauri continuously from UT 1551 on 22 August, 1985 to UT 1954 on 23 August, 1985, covering 2.24 binary orbits, including two white dwarf eclipses. During this time, 26.9 hours of data were obtained by the CMA at the focus of the LE1 telescope (Korte et al. 1981), which is sensitive in the 0.03-2.5 keV bandpass. The thin lexan, aluminum, thick lexan, and boron filters were used. V471 Tau was detected in all but the boron filter. A weak 2-6 keV flux was detected by the medium energy (ME) detectors. We defer a report on this harder X-ray flux to a forthcoming paper.

a) Soft X-rays from Both Stars – The LE light curve for the entire observation is shown in Figure 1. The decline in the soft X-ray flux during the white dwarf eclipse phases, centered at phases 1.0 and 2.03, indicates that most of this flux comes from the white dwarf. The eclipse light curve is more clearly illustrated in Figure 2, which also shows a residual soft X-ray flux from the K star. The sharpness of the X-ray eclipse is consistent

with the 1 minute interval between optical contacts (Beavers, Oesper, and Pierce 1979). The count rates observed or estimated from each star in each of the four filters are given in Table 1.

b) Soft X-ray Dips -- Pronounced dips in the soft X-ray flux at orbital phases 0.15, 0.18, and 0.85 can be seen in the LE light curve (Figure 1). The phase 0.85 event is the strongest, with essentially complete cutoff of the white dwarf flux at the depth of the event. It occurs relatively unchanged for three successive binary orbits. The phase 0.15 event occurs during the first orbit, but is gone 12.5 hours later. The phase 0.18 event also occurs during the first orbit, and is greatly diminished 12.5 hours later. There is also a broader, more shallow flux decrease between phases 0.62 and 0.83 during the second orbit. This decrease does not occur during the next orbit. The eclipse light curve (Figure 2) shows a lower observed flux level before the first eclipse ingress (top). During the next eclipse ingress (bottom), the flux has returned to the 'clean' level. The egress light curves, also shown in Figure 2, are characterized by sharper dips occurring between phases 0.04 and 0.06.

c) White Dwarf Pulsations - A Fourier analysis of the LE flux has revealed a 9.25 minute periodic variation (Jensen 1985). A power spectrum for data obtained for the 'clean' phases 0.22 - 0.62 is shown in Figure 3. There is more power in the first harmonic at 3.604 mHz than in the 1.802 mHz period. The inset in Figure 3 shows the pulse profile for the subset of 'clean' data obtained with the thin lexan filter. The pulse profile is double peaked, accounting for the strength of the first harmonic. The count rate at pulse minimum is ~80% of the count rate at pulse maximum.

III. DISCUSSION

a) The X-ray Fluxes - The soft X-ray fluxes from white dwarfs have generally been successfully fit by photospheric models (Kahn et al. 1984; Heise 1985; Petre, Shipman, and Canizares 1986). The white dwarf rates listed in Table 1 were fit by white dwarf model atmospheres for T_{eff} = 30000 K, 32500 K, and 35000 K, and log g = 8.0 and 8.5 to test the possibility that the soft X-ray flux from the white dwarf in V471 Tau is photospheric in origin. Details concerning the model atmospheres we used can be found in Petre, Shipman, and Canizares (1986). Since the photospheric temperature, gravity, and distance to the source are already approximately known, the observed EXOSAT count rates for the three filters provide a good constraint on the chemical composition of the photosphere and the interstellar column density. To model the composition of the photosphere, we varied the helium abundance as log N[He/H] = -5.3 to -3.7 in steps of 0.1 dex. A pure hydrogen atmosphere model was also tested. We have assumed a negligible opacity due to metals heavier than helium. Simulations show that metal abundances less than 10^{-3} solar produce a negligible opacity (Kahn et al. 1984). IUE observations of V471 Tau have not constrained metal abundances in this range. Until more sensitive UV spectra are obtained, we cannot rule out the possibility that photospheric metal opacity has an effect on the emergent soft X-ray flux.

The results from our fits are summarized in Table 2. Successful fits are found for T_{eff} = 35000 K and log g = 8.0 and 8.5. A T_{eff} = 32500 K, log g = 8.5 model almost fits, suggesting that a finer grid of models would show a slightly higher temperature to be within acceptable bounds. The

agreement between the EXOSAT data and white dwarf model atmospheres, for temperatures and gravities consistent with UV observations, provides evidence that the soft X-ray flux from the white dwarf in V471 Tau originates in a $T_{eff} \sim 35000$ K photosphere which may contain trace elements of helium and/or heavier metals. The successful photospheric models give a 0.03-2.5 keV white dwarf flux of $3 +/- 1 \times 10^{-11}$ ergs cm^{-2} s^{-1}, corresponding to a luminosity of $4 +/- 1 \times 10^{31}$ ergs s^{-1}. Because the white dwarf flux is pulsed, it is probable that a fit of a homogenous photospheric model to the pulse averaged count rates does not correctly constrain the 'average' photospheric parameters. Additional fits of more complex photospheric models are in preparation.

The K star has a migrating RS CVn type wave (Young et al. 1983, and references therein), which implies spotted regions and a high density of magnetically confined coronal plasma. Its corona is presumably similar in nature to those of other late type stars observed by the Einstein and EXOSAT Observatories, and describable in terms of thermal emission with kT in the range 0.3-2 keV (e.g. Golub 1983). The observed ratio of rates in the thick and thin lexan filters is consistent with temperatures in this range for interstellar column densities of $1-7 \times 10^{18}$ cm^{-2}, which are also consistent with the white dwarf models. The implied 0.03-2.5 keV K star flux is $\sim 6 \times 10^{-12}$ ergs cm^{-2} s^{-1}, corresponding to a luminosity of 1.8×10^{30} ergs s^{-1}.

b) The Dips - The lines of sight to the white dwarf during the dips are illustrated in Figure 4. Material located along these lines of sight was at least 2-3 stellar radii from the K star. The dips at phases 0.62 to 0.75 must be due to material located closer to the white dwarf than to the K

star.   Figure 4 shows that the dips at phases 0.15, 0.18, and 0.85 occurred when the triangular ~~(outer)~~ Lagrangian points of the binary orbit are near the line of sight to the white dwarf.   These unique phases are 0.83 for the Lagrangian point on the ingress side (L4) and 0.17 for the point on the egress side (L5) (Kopal 1978). Possibly ejected material can   collect at these potential minima for at least several binary orbits. Alternatively, the material could be in very large coronal loops anchored to the K star. Another possibility is that absorbing material is located at greater, circumbinary distances. Sion and Bruhweiler (1986)   have suggested the presence of cool circumbinary material in this system.

No 9   Absorption dips in neutron star low mass binary systems have been attributed to structures related to accretion disks (e.g.   White and Mason 1986).   There is no evidence in the V471 Tau UV data for an accretion disk (Guinan and Sion 1984).

The sharp dips between phases 0.04 and 0.06 on the egress side of the eclipse are likely to be due to material bound to the K star.. The event at phase 0.052 during the first eclipse (top), if due to material in a cool K star loop, would require a loop height of ∼0.2 stellar radii.   The variability we observe in the soft X-ray light curve near the eclipse therefore suggests that dense, cool loops with heights ∼0.2 stellar radii are present on the K star, and are variable in density and/or temperature on a time scale shorter than 12.5 hours.   The transient C IV absorption line observed by IUE near the eclipse phase (Guinan and Sion 1984) is consistent with the presence of such structures.

c) The White Dwarf Pulsations - We consider the most likely cause of the pulsations to be either 1) the rotation of a non-homogenous photosphere, with the inhomogeneity produced by mass accretion onto magnetic polar regions of the white dwarf, or 2) nonradial g mode oscillations excited by an instability in the photosphere.

i) Rotation? - The double peaked pulse profile is suggestive of a bipolar structure in the white dwarf photosphere, which could be readily explained if it is accreting mass from the K star onto magnetic polar regions. The mass accretion rate should determine whether the poles are bright or dark in X-rays. For example, a rate of $10^{-11.5} M_\odot yr^{-1}$ could produce 12.5 eV polar hot spots with a filling factor of $10^{-3.5}$. A blackbody flux from such spots would be consistent with the EXOSAT data, and is an alternative to the photospheric models, but the required accretion rate is high for a detached binary in which the mass transfer is through capture of the K star wind. Accretion rates $< 10^{-12} M_\odot yr^{-1}$ would not produce polar hot spots bright enough to modulate the soft X-ray flux, but may supply sufficient helium or metals to produce dark spots. Sion and Starrfield (1984) have suggested that the photospheric metal lines observed in the hot DAZ white dwarf Feige 24 are supplied in this fashion from the detached M dwarf companion. The white dwarf magnetic field strength does not have to be as high as the fields in magnetic cataclysmic variables to be able to channel these lower accretion flows onto the poles.

ii) Oscillations? - The instability of white dwarf photospheres to nonradial g mode oscillations, excited by the κ-mechanism in partial ionization zones, is well established for DA white dwarfs sufficiently cool

(T_{eff} < 12000 K) to have unstable hydrogen partial ionization zones, the ZZ Ceti variables (Winget et al. 1982a). The discovery of DB pulsators with T_{eff} ~ 30000 K (e.g. GD358, Winget et al. 1982b, and PG1654+160, Winget et al. 1984) confirms the existence of a helium instability strip near this temperature. Given the extreme sensitivity of the temperature of the helium instability strip to the efficiency of convection (Winget et al. 1983), it is possible that DA white dwarfs with T_{eff} ~ 35000 K and a stratified H/He atmosphere could be unstable to nonradial g mode oscillations driven by a helium partial ionization zone beneath a thin hydrogen surface layer. Cox and Starrfield (1986) and Kawaler (1986) have recently argued that nonradial g mode oscillations in hot DA white dwarfs could be driven by nuclear burning.

Additional EXOSAT observations of V471 Tau in February 1986 confirm the existence of the 9.25 minute pulsations. The pronounced dips, which were prominent in the August 1985 observation, were not evident in the February 1986 observations. A more detailed analysis and discussion of all of the EXOSAT observations of V471 Tau will appear in a forthcoming paper.

References:

Beavers,W.I., Oesper,D.A., and Pierce,J.N. 1979, Ap.J.(Letters), 230, L187.

Cox,A.N. and Starrfield,S.G. 1986, ????

Golub,L. 1983, in I.A.U. Colloq. No. 71, "Activity in Red Dwarf Stars", ed.
    P.B.Byrne and M.Rodono (Dordrecht : Reidel), p.83.

Guinan,E.F. and Sion,E.M. 1984, _Astron.J._, _89_, 1252.

~~Hall Reference ????~~

Hamada,T. and Salpeter,E.E. 1961, _Ap.J._, _134_, 683.

Heise,J. 1985, _Space Sci. Rev._, _40_, 79.

Henry,R.B.C., Shipman,H.L., and Wesemael,F. 1985, _Ap.J.Suppl._, _57_, 145.

Jensen,K.A. 1985, I.A.U. Circular No. 4?02.

Kahn,S.M. et al. 1984, _Ap.J._, _278_, 255.

Kopal,Z. 1978, _Dynamics of Close Binary Systems_, Dordrecht, Reidel.

Korte, de P.A.J. et al. 1981 _Space Sci. Rev._, _30_, 495.

Petre,R., Shipman,H.L., and Canizares,C. 1986, _Ap.J._, ~~submitted~~ _304_, in press.

Sion,E.M. and Bruhweiler,F.C. 1986, ??????

Sion,E.M. and Starrfield,S.G. 1984, _Ap.J._, _286_, 760.

Van Buren,D., Charles,P.A., and Mason,K.O. 1980, _Ap.J.(Letters)_, _242_, L105.

Vandenberg,D.A. and Bridges,T.J. 1984, _Ap.J._, _278_, 679.

White,N.E. and Mason,K.O. 1985, ~~?????~~ _Space Sci. Rev._, _40_, 167.

Winget,D.E. et al. 1982a, _Ap.J.(Letters)_, _252_, L65.

Winget,D.E. et al. 1982b, _Ap.J.(Letters)_, _262_, L11.

Winget,D.E. et al. 1983, _Ap.J.(Letters)_, _268_, L33.

Winget,D.E. et al. 1984, _Ap.J.(Letters)_, _279_, L15

Young,A. and Capps,P.W.. 1971, _Ap.J.(Letters)_, _166_, L81.

Young,A. and Nelson,B. 1972, _Ap.J._, _173_, 653.

Young,A. et al. 1983, _Ap.J._, _267_, 655.

TABLE 1. EXOSAT LE COUNT RATES for V471 TAURI

Filter	Total Rate (s^{-1})	K Star Rate (s^{-1})	White Dwarf Rate (s^{-1})
Thin Lexan	1.093 ± 0.014	0.0456 ± 0.0063	1.047 ± 0.016
Thick Lexan	0.636 ± 0.010	0.0319 ± 0.0154	0.604 ± 0.018
Aluminum	0.810 ± 0.011	0.0182 ± 0.0073 [2]	0.792 ± 0.013
Boron [2]	< 0.009	< 0.009	< 0.009

1 - Estimated from the thin lexan rate, using 0.3-1.0 keV thermal spectra with $\log N_H = 18.7$

2 - No detection. Upper limit is 3σ. Distinction between the K star and white dwarf is not possible.

TABLE 2.

WHITE DWARF MODEL ATMOSPHERE FITS to EXOSAT LE DATA

T_{eff} (K)	$\log g$	Successful fit?	$\log N_H$ (cm^{-2})	$\log(N[He/H])$
30,000	8.0	No	—	—
30,000	8.5	No	—	—
32,500	8.5	Almost	~ 18.5	Pure Hydrogen
35,000	8.0	Yes	18.69 ± 0.02	-4.6 ± 0.07
35,000	8.5	Yes	18.77 ± 0.03	< -5.4

FIGURE 1 - Light curve of the 0.03-2.5 keV flux from V471 Tauri for th entire 28 hour observation. The time bins are 554.85s, equivalent to on. white dwarf pulse period. The data from the thick lexan and aluminum filter: are normalized with respect to the thin lexan filter rate (cf Table 1), and combined with the thin lexan filter data to produce a light curve approximately equivalent to that which would be obtained from a continuous observation with the thin lexan filter. The horizontal dashed line indicates the mean thin lexan count rate between orbital phases 0.22 and 0.62. The vertical dashed lines mark the phases of quadrature. The phases at which the *triangular* ~~outer~~ Lagrangian points (L4 and L5) are in our line of sight to the white dwarf are indicated by the arrows. The white dwarf is eclipsed at phases 1.0 and 2.0.

FIGURE 2 - Light curve of the 0.03-2.5 keV flux from V471 Tauri for the two eclipses of the white dwarf. The time bins are 115.6s out of eclipse and 554.85s during eclipses. The top figure shows the first eclipse. The bottom figure shows the second eclipse. All of the data shown were obtained using the thin lexan filter except for phases 0.9-1.01 during the first eclipse, which is thick lexan filter data. This data has been normalized to a level common with the thin lexan filter data. The data are also normalized with respect to a pulse profile template, so that the short time scale variability is not due to the pulse variability.

FIGURE 3 - Power spectrum of the 0.03-2.5 keV flux for all data collected between orbital phases 0.22 and 0.62. The data from the thick lexan and aluminum filters are normalized with respect to the thin lexan filter rate, and combined with the thin lexan filter data to produce the input time

series. The power is normalized with respect to the Poisson noise level. The Nyquist frequency is 86.51 milliHertz (mHz). The frequency resolution is 0.01056 mHz. The higher frequency power (unshown) is completely consistent with a Poisson noise process. The two horizontal dashed lines indicate the minimum power levels for which features exceed Poisson noise expectations at confidences of 50% and 99%.

FIGURE 4 - Schematic of the V471 Tauri binary system, indicating the orientations of the five Lagrangian points, and their Roche equipotentials, with respect to the white dwarf and K star components. A mass ratio q=1 is used. The K star clearly does not fill its Roche lobe. The curved arrows indicate the sense of rotation of the system. The dotted lines mark the orbital phase range for which dips are seen in the 0.03-2.5 keV light curve. The lines of sight to the white dwarf at the ~~outer~~ triangular Lagrangian phases (0.167 and 0.833) are indicated by dashed lines, as is the eclipse phase 0.0. The shaded regions indicate the phases at which dips are seen. The dip near the L4 point is particularly deep and persistent, and is therefore more heavily shaded.
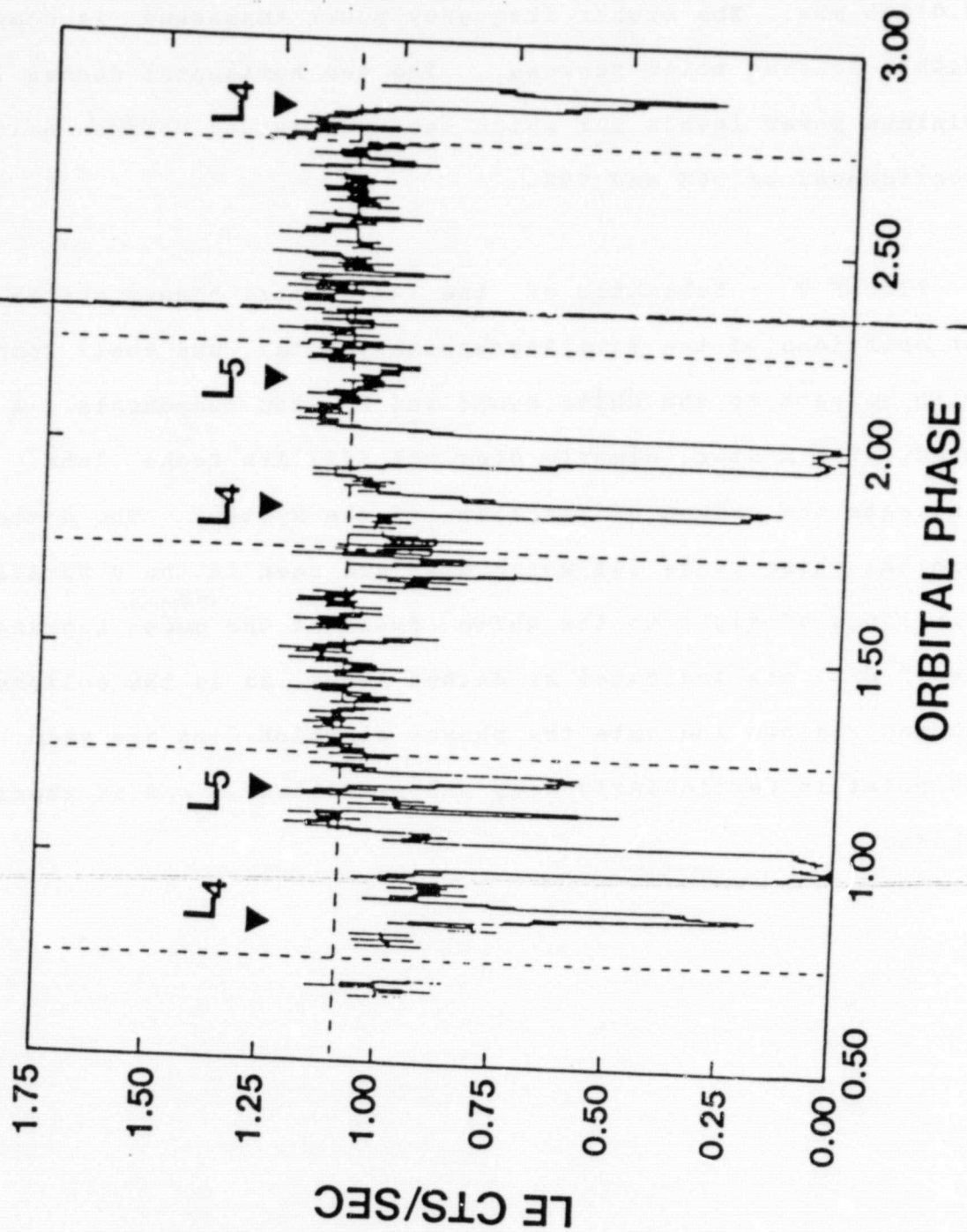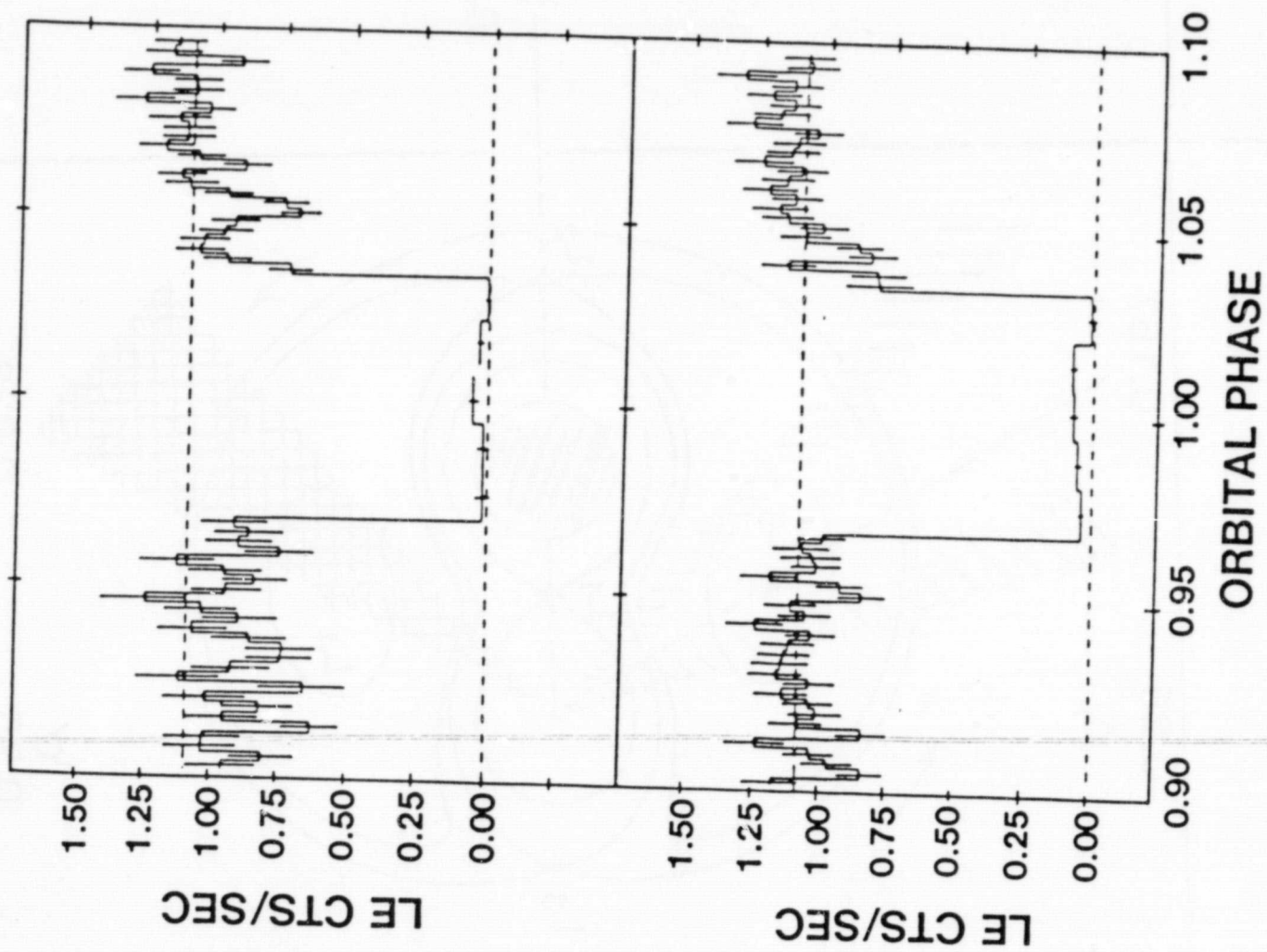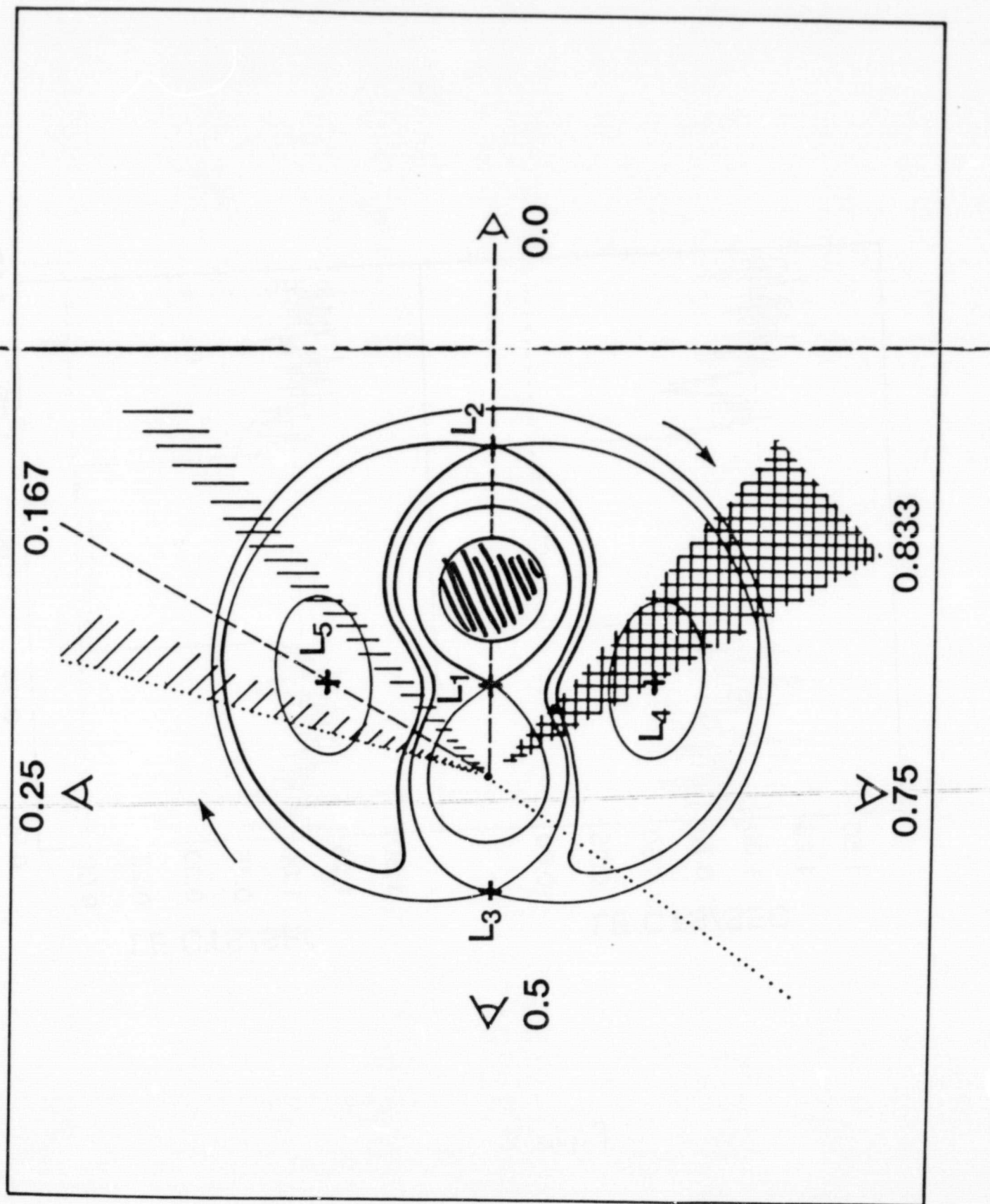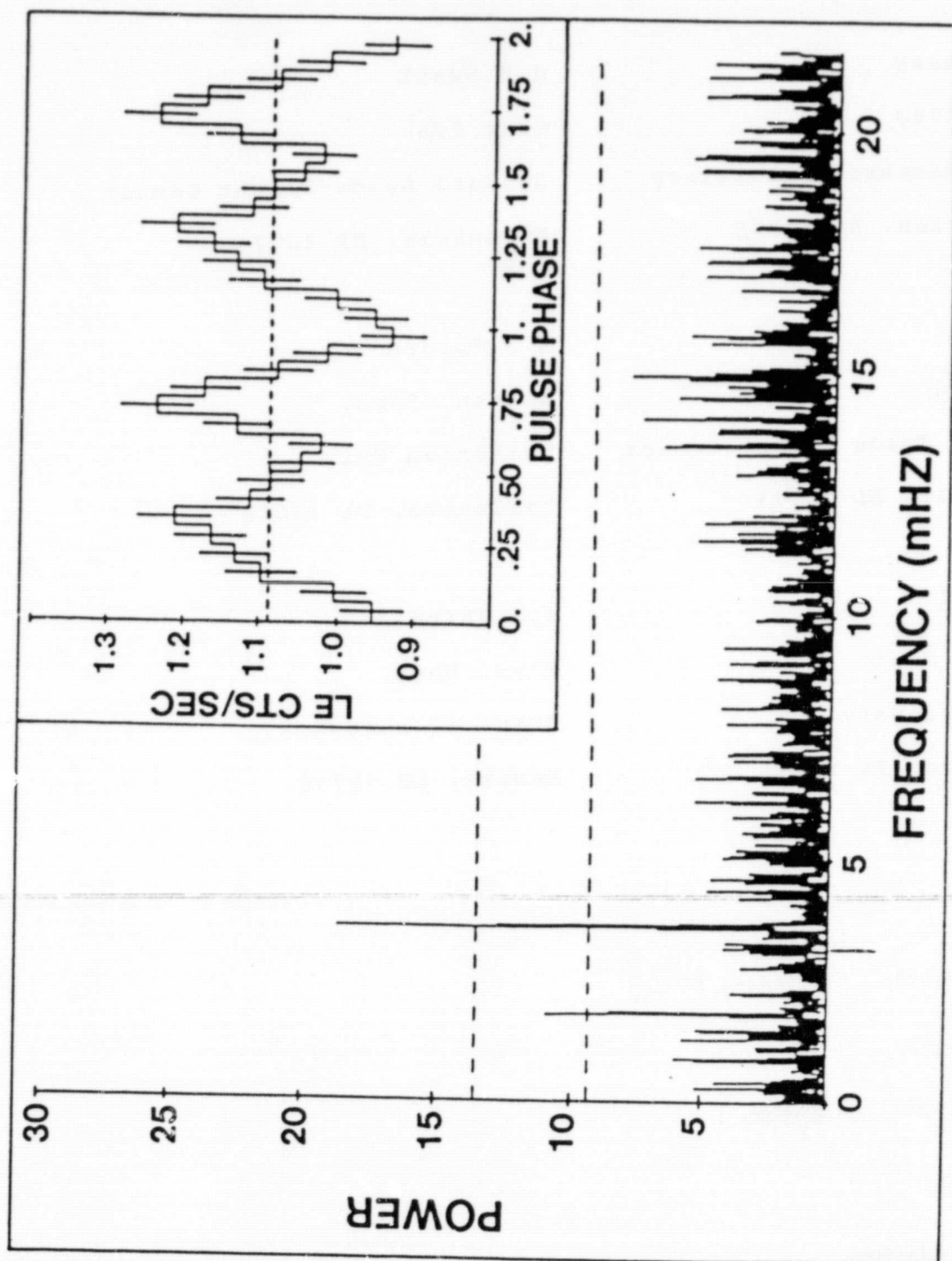
Figure 1

Figure 2

Figure 3

Figure 4

Addresses:

K.A.Jensen

Code 4170J

Naval Research Laboratory

Washington, DC 20375

R.Petre

Code 666

Goddard Space Flight Center

Greenbelt, MD 20771

E.M.Sion

Astron. Dept.

Villanova Univ.

Villanova, PA 19085

J.H.Swank

Code 666

Goddard Space Flight Center

Greenbelt, MD 20771

E.F.Guinan

Astron. Dept.

Villanova Univ.

Villanova, PA 19085

H.L.Shipman

Phys. Dept.

Univ. of Delaware

Newark, DE 19716

2380 words (including titles)

+ References

+ 4 Figures (and captions)

+ 2 Tables

+ Authors' Addresses

Temperature, radius and rotational velocity of Sirius B.

by Peter Thejll and Harry L. Shipman.
Physics Department, University of Delaware,
Newark, Delaware 19716.

Abstract.

Based on the theoretical work, by Ostriker and Hartwick (1968), concerning the magnetic fields of rotating white dwarfs, and the recent determination of the effective temperature, by Holberg et al. (1984), we have derived the interrelationships between radius, rotational velocity and effective temperature for Sirius B.

We find that i) the radii, 0.76 to 0.81 in hundredths of solar radii, predicted by T_{eff} between 26000 and 28000K and a mass of $1.05M_o$ places Sirius B somewhat above the Hamada-Salpeter mass-radius relation, by about 1 or 2 σ. ii) the rotational velocity of Sirius B is predicted to lie between 0 and 600 km/s (using 2 σ limits) and that only radii which place a white dwarf above the mass-radius line are allowed. iii) in order to further limit the rotational velocity and the radius of Sirius B better determinations of T_{eff} and magnitude are needed. If the satellite HIPPARCOS can determine the parallax of Sirius B with 1 milliarcsecond accuracy then the errors on T_{eff} and the magnitude will be the limiting factors in the future.

Keywords: Sirius B - rotating white dwarfs - magnetic fields - Mass/Radius relation.

I. Introduction.

The motivation for our work is twofold. We want to check if Sirius B falls on the mass-radius (M-R) relation using new data from Holberg et al. (1984). Only a few objects have so far been placed conclusively on that relation. We also wish to present a new method for determining rotational velocities for cases when the standard method, of modeling rotationally-broadened lines, doesn't work.

Many determinations of Sirius B's properties have been made over the years. Greenstein, Oke and Shipman (1971) analyzed the H_α and H_γ line profiles and arrived at $T_{eff} = 32000$ +/- 1000K, along with gravity and radius: $R/R_o = 0.0078$ +/- 0.0002. Shipman (1976) pointed out that a pure Hydrogen model with $T_{eff} = 32000K$ would have the low absorption coefficient in the X-ray region necessary to explain the X-ray observations by Mewe et al. (1975). This value of T_{eff} was obtained using unblanketed model atmospheres. If blanketed atmospheres had been used, this value of T_{eff} would have been lowered by 2000K. Later determinations of T_{eff} have confirmed the general conclusion that Sirius B is much hotter than Sirius A, but also lowered the T_{eff} somewhat. Bohm-Vitense, Dettman and Kapranidis (1979) found $T_{eff} = 26000$ +/- 1000K by fitting theoretical models to IUE spectra of Sirius B. Later Martin, Basri and Lampton (1982) used HEAO1 A-2 data and fitted a 28000K model finding support for a photospheric origin of the X- rays. Using the IUE data and UV data from Voyager 2 Holberg, Wesemael and Hubeny find support for T_{eff} in the range 26000 - 28000K with a firm upper limit at 28000K. EXOSAT data will also provide a constraint on the T_{eff} although

uncertanties in the EXOSAT calibration are still being investigated.

One open question is whether, given all these determinations of T_{eff}, Sirius B fits on the M-R relation. One reason Sirius B might not fit the mass- radius relation is that rotation can increase its radius (Ostriker and Hartwick, 1968). While one can analyze the rotationally broadened line profiles (Pilachowski and Milkey, 1984) this method is only applicable to stellar spectra with very high resolution - and thus only useful for a few bright stars. Another possibility is that residual nuclear burning could increase the radius from its zero temperature value, as has been shown by Koester and Schonberner (1986) for 0.6 M_o stars. A similar calculation for the $1M_o$ case has not been done, but the effects of nuclear burning would be smaller, and possibly negligible, for a higher mass.

Ostriker and Hartwick established the relationship between radius, magnetic field and angular momentum for a white dwarf of mass $1.05M_o$. We can use their work to get the relationships between radius, rotational velocity and temperature, provided that we have an upper limit to the magnetic field strength and have values for orbital elements, the magnitude and the parallax. We have applied this method to Sirius B.

II. Method.

From Keplers third law one can calculate the total mass of the Sirius system and use the accurately known fractional mass of Sirius B to find its mass. The radius of Sirius B is found by using the calculated relationship between absolute flux and effective temperature (Shipman 1979, table 2) and the magnitude and parallax (Gatewood and Gatewood, 1978). In using the Ostriker and Hartwick (1968) results we assume that Sirius B rotates as a homogeneous sphere and that there is essentially no magnetic field on Sirius B. We base this last assumption on inspections of high-resolution spectra of the H_α and H_γ lines (Greenstein, Oke and Shipman, 1971, unpublished spectra).

As we used Ostriker and Hartwicks results we found that the $v_{eq}=0$ line fell above the Hamada-Salpeter mass-radius relation. We assume this is because Ostriker and Hartwick did not sufficiently model the envelope of white dwarfs and that if they had done so the $v_{eq}=0$ line would have fallen on the Hamada Salpeter M-R relation. Thus we put $v_{eq}=0$ on the M-R line for a C^{12} body. We assumed the angular momentum of Sirius B could be modeled by using the moment of inertia of a homogeneous sphere. Using a more realistic mass distribution ($\rho(r)r^2=$const.) makes only a 20% difference in the equatorial rotational velocity v_{eq}.

In fig.1. we plot the results of our analysis in a M-R diagram. We have drawn lines parallel to the Hamada-Salpeter relation through each point determined by velocity and mass - we are thus assuming that the M-R lines for non-zero velocities will look like this in a small area close to the HS line. Fig.2 is a more detailed nomogram where the relationships between T_{eff}, radius and rotational velocities can be seen for a $1.05M_o$, homogeneous, spherical white dwarf.

III. Uncertainties.

The quantities that enter our calculations are of course in error to some extent - to see how important these errors are we both calculated the propagation of errors and introduced 1σ shifts in the parallax and the magnitude to see the effects. (See fig. 1.) The sizes of the relative errors σ_{rel} on the quantities that determine the mass of Sirius B are:

$$(\sigma_{rel}(M_B))^2 = (3\sigma_{rel}(\pi))^2 + (3\sigma_{rel}(\alpha))^2 + (\sigma_{rel}(f_B))^2 + (2\sigma_{rel}(P))^2$$

or

$$(0.0261)^2 = (0.0246)^2 + (0.0079)^2 + (0.0030)^2 + (0.0022)^2$$

where π, α, f_B and P are; parallax, angular semi-major axis of the orbit, the fractional mass of Sirius B and the period of the orbit. The 3% error is mainly due to the error on the parallax, α contributes about one tenth as much.

The error on the radius, determined from $H(T_{eff})$, π and magnitude m, is dominated by the error on the magnitude:

$$(\sigma_{rel}(R_B))^2 = (\ln 10/5 \ m \ \sigma_{rel}(m))^2 + (\sigma_{rel}(\pi))^2 + (\sigma_{rel}(H(T_{eff})/2))^2$$

or

$$(0.0192)^2 = (0.0166)^2 + (0.0082)^2 + (0.005)^2$$

where we have assumed that the relative error on $H(T_{eff})$ is 1% - a reasonable number, as will be discussed in section IV. The error on the magnitude contributes about four times as much as does the error on the parallax. We have used an absolute error on the magnitude of $(0.03)^2 + (0.02)^2$ where the last term takes into consideration the absolute calibration error. It is obvious that an improved determination of the magnitude is called for. Perhaps it is impossible, at the present epoch of the Sirius B orbit, and with standard techniques, to improve significantly on the value for the magnitude, but, as Smith and Terrile (1984) point out in their paper on the β Pictoris disk the sort of equipment they used is very well suited for photometric work near bright sources, such as the Sirius system.

How will the capabilities of the HIPPARCOS satellite change matters? If it can determine parallaxes to within 1 milliarcsecond then the error on M_B that π introduces will be the same as that from the semi-major axis and furthermore the uncertainty on the magnitude will overshadow that on the parallax by a factor of nearly 40 in its influence on the relative error of R_B.

C-2

IV. Discussion of the methods.

We determine the radius R of Sirius B by using the fundamental relation between the stellar flux f, the monochromatic Eddington flux at the stellar surface $H(T_{eff})$, and the stellar distance D, from Shipman 1979:

$$(1) \quad R = D \ (f/(4\pi H(T_{eff})))^{1/2}$$

Because of the sensitivity of the results we discuss to relatively small uncertainties in the values of various input quantities, we include a considerable discussion of the above equation and the uncertainties therein, and ask for the readers' patience with what is in places a pedagogical discussion. Earlier discussions of errors have been given by Shipman (1979) and, with respect to the accuracy of the $H(T_{eff})$ relation, by Wesemael et al. (1980).

An advantage of this method, and of all surface brightness methods for determining a stellar radius, is that you do not need to know (or guess) how much energy the star is emitting at all wavelengths. The disadvantage is that you must be able to determine the stellar flux H accurately. But this problem can be circumvented or minimized by carefully choosing the wavelength or wavelength range over which you fit the above equation to the data. Provided that you apply the equation at a wavelength which is shortward of the Planck maximum, the dependence of H on T_{eff} is relatively weak - linear in the black-body approximation - which minimizes the uncertainty in R produced by uncertainties in T_{eff}.

In this paper we apply it in the V band, since the V flux from Sirius B is known to within 0.03 magnitudes. In contrast, Bohm-Vitense et al. applied the equation in the IUE spectral range, which one might think to be superior, being closer to the Planck maximum at these temperatures. However, model calculations indicate otherwise. $H_{5405 A}$ increases by 33% when you increase T_{eff} from 30,000K to 35,000 K, while $H_{1363 A}$ increases by 57% (Shipman, unpublished, blanketed, non-LTE models; the Wesemael et al. models are virtually identical, as is shown in table 1). Thus, a 1,000 K uncertainty in T_{eff} produces an uncertainty of 6.6% in H (and 3.3% in R) when you use this method in the V band, and an uncertainty of 11% in H (5.5% in R) when you use the method in the IUE spectral range. This consideration, by itself, suggests that the visual band is the one to work with.

The ultraviolet spectral band is not as useful for application of equation (1), although it is essential if one is to determine T_{eff} accurately. The correction for scattered light in the IUE spectral range is considerable, being smallest at the shortest wavelengths, and is uncertain, since one has to use an existing spectroscopic instrument rather than a specially constructed area scanning photometer. In addition, the uncertainty in the overall IUE absolute calibration is usually quoted at 10% (see, e.g., R.C. Bohlin, et al., 1980 and R.C. Bohlin, 1985). Individual readers can make their own judgments of the accuracy of the IUE measurements of the Sirius B UV flux, but it is at least as uncertain as

the overall calibration uncertainty of 10%. Our examination of the figures in Böhm-Vitense et al. suggests that the uncertainty in measuring f generated by the need for correcting for scattered light is probably half of the total correction, or, at the shortest wavelengths, about 15%, producing an overall error in f of $(10)^2 + (15)^2$ or 18%, which corresponds to 9% in R arising from uncertainties in the flux measurements alone, if you apply equation (1) in the IUE spectral range.

An additional consideration which must be applied in an investigation of this kind is how good are the models; how well can you trust the $H(T_{eff})$ relation which enters equation (1) ? This point has been discussed earlier by, e.g., Auer and Shipman (1977), Shipman (1979b) , and most extensively by Wesemael et al. (1980). The ATLAS program, used for the $H(T_{eff})$ relation used here (and in Shipman 1979), and the Auer-Mihalas program as modified by Wesemael, used for the Wesemael et al. calculations, are completely independent. The uncertainties in $H_{5405\,A}$ for a given T_{eff} are really quite small (see table 2.); at T_{eff} = 20,000 K, comparing blanketed models with blanketed models, the relative change in H_{5405} calulated as $(H_{Shipman} - H_{Wesemael}/H_{Shipman})$ is +0.0059, at T_{eff} = 30,000 K it is -0.0032 and it is -0.0061 at T_{eff} = 50,000 K. Using unpublished, non- LTE models calculated at Delaware indicates a realtive change in $H_{5405\,A}$ calculated as $(H_{nonLTE} - H_{LTE})/H_{LTE}$ = 0.011 at 35,000 K. This scale is quite gravity independent; going from log(g) of 8 to 8.5 at 30,000 K decreases the Eddington flux, in these same relative terms, by -0.0082. The uncertainties in the $H(T_{eff})$ relation are thus far smaller than that of the magnitude and can safely be estimated at about 1% or less.

V. Results.

On fig. 1 one sees that the temperature range that Holberg et al. arrived at corresponds to a range in radii of from 0.76 to 0.81 in $100R/R_o$. This is above the C^{12} mass-radius relation of Hamada and Salpeter, but if 1σ shifts are introduced in magnitude, mass and parallax then Sirius B moves onto the M/R relation. Not until the errors on magnitude, parallax and of course T_{eff} are reduced, as discussed above, can the issue of Sirius B's placement on or off the mass-radius relation be settled.

From the Holberg et al. temperatures and the Ostriker and Hartwick results we find the velocity to lie between 0 and 600 km/s - these are the velocity limits that a 2σ circle, centered at (M,R), touches. Furthermore, only positive rotational velocities are allowed, so only the part of the M-R plane above the C^{12} line is accessible. Any temperature and mass determinations that place Sirius B, or any other white dwarf, below the line can thus be ruled out.

VI. Discussion.

Some interesting considerations, and some suggestions for current work, emerge from a consideration of how the astrometric data on Sirius are likely to improve in the future. The European satellite HIPPARCOS can improve the parallax of Sirius significantly; the current best parallax (Gatewood and Gatewood, 1978) has an uncertainty of 3 milliarcseconds, and the advertised HIPPARCOS capability should improve this by a factor of 3. Such improvement can, in principle allow us to determine the radius with much greater precision than we can now. In addition, at the present time the uncertainty

in the mass is dominated by the uncertainty in the parallax; with a perfect parallax, the uncertainty in the relative orbit produces a mass with an uncertainty of 0.9% (compared with the current value of 2.5%), where the uncertainty in the relative orbit contributes equally to the total uncertainty in the mass.

At that time this analysis can be done with considerable more precision, if our estimates of the temperature, and of the visual magnitude, or the absolute flux at any wavelength, of Sirius B, can be improved significantly over the present values. At the moment, the uncertainty in parallax, temperature, and visual magnitude all contribute roughly equally to the uncertainty in the radius; in the future, the magnitude and temperature will dominate. This suggests that continued efforts to improve the accuracy of particularly the visual magnitude and of the temperature of the companion will be worthwhile.

$T_{eff}\backslash\lambda$	5405 A	1363 A
30,000 K	3.41e-4	1:98e-3
35,000 K	4.545e-4	3.116e-3
[H(35)-H(30)]/H(30)	0.333	0.574
$\Delta T=1000$ K	$\Delta H=0.067$	$\Delta H=0.115$
	$\Delta R=0.033$	$\Delta R=0.057$

Table 1: Showing the sensitivity of $H(T_{eff})$ to changes in T_{eff} in the V band and the IUE spectral range. The sensitivity is least in the V band. From unpublished models by Shipman.

T_{eff}	HS	Wesemael et al.	HS log(g)=8.5
20,000 K	1.70e-4	1.69e-4	(+0.005)
30,000 K	3.41e-4	3.421e-4	(-0.0082)
50,000 K	6.49e-4	6.58e-4	(+0.013)

Table 2: Showing $H_{5405 A}$, as calculated by Shipman and Wesemael et al. using completely different programs, for different T_{eff} and log(g). The first two coloumns are for log(g)=8 and the last is for the change in H when going from a log(g)=8 to a log(g)=8.5 model, relative to the log(g)=8 model. Note the very small dependencies of H on log(g) and choice of program. Modified from Table 1 of Wesemael et al. 1980.
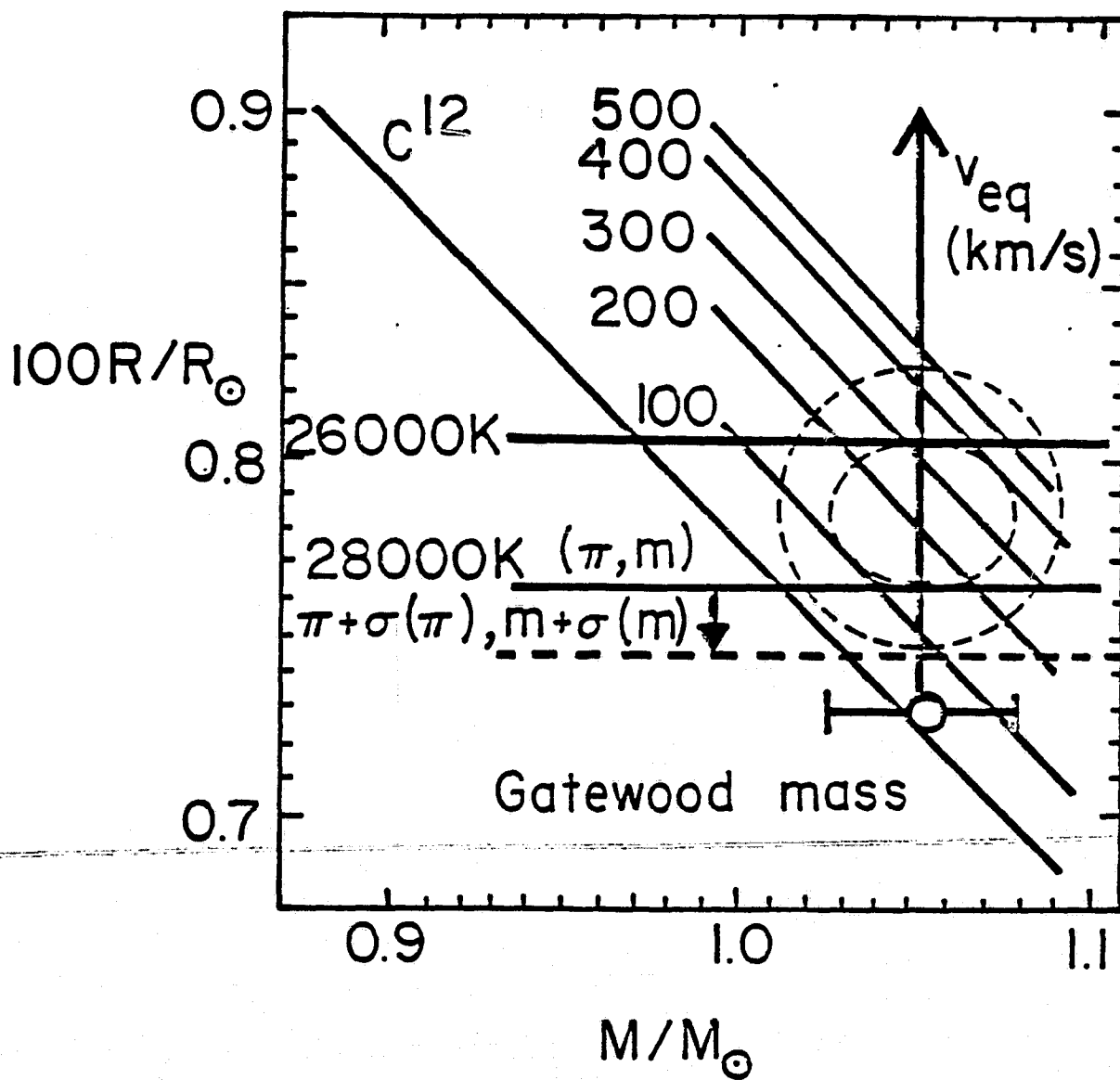
Fig.1. Mass-Radius diagram for a 1.05 M_0 white dwarf, like Sirius B. The line marked C^{12} is the Hamada-Salpeter zero temperature mass-radius relation and the two horizontal lines represent the radii calculated from the upper and lower limits on T_{eff} set by Holberg et al. Astrometric data and the magnitude was taken from Gatewood and Gatewood. If 1 sigma shifts are introduced in the magnitude and the parallax the radius-line given by 28000K moves down to the dashed line, showing the influence of errors on the input data. The velocity scale gives the equatorial rotational velocity in km/s for a homogenous, spherical body, modified from data given by Hartwick and Ostriker. The two circles have radii 1 and 2 sigma, respectively.
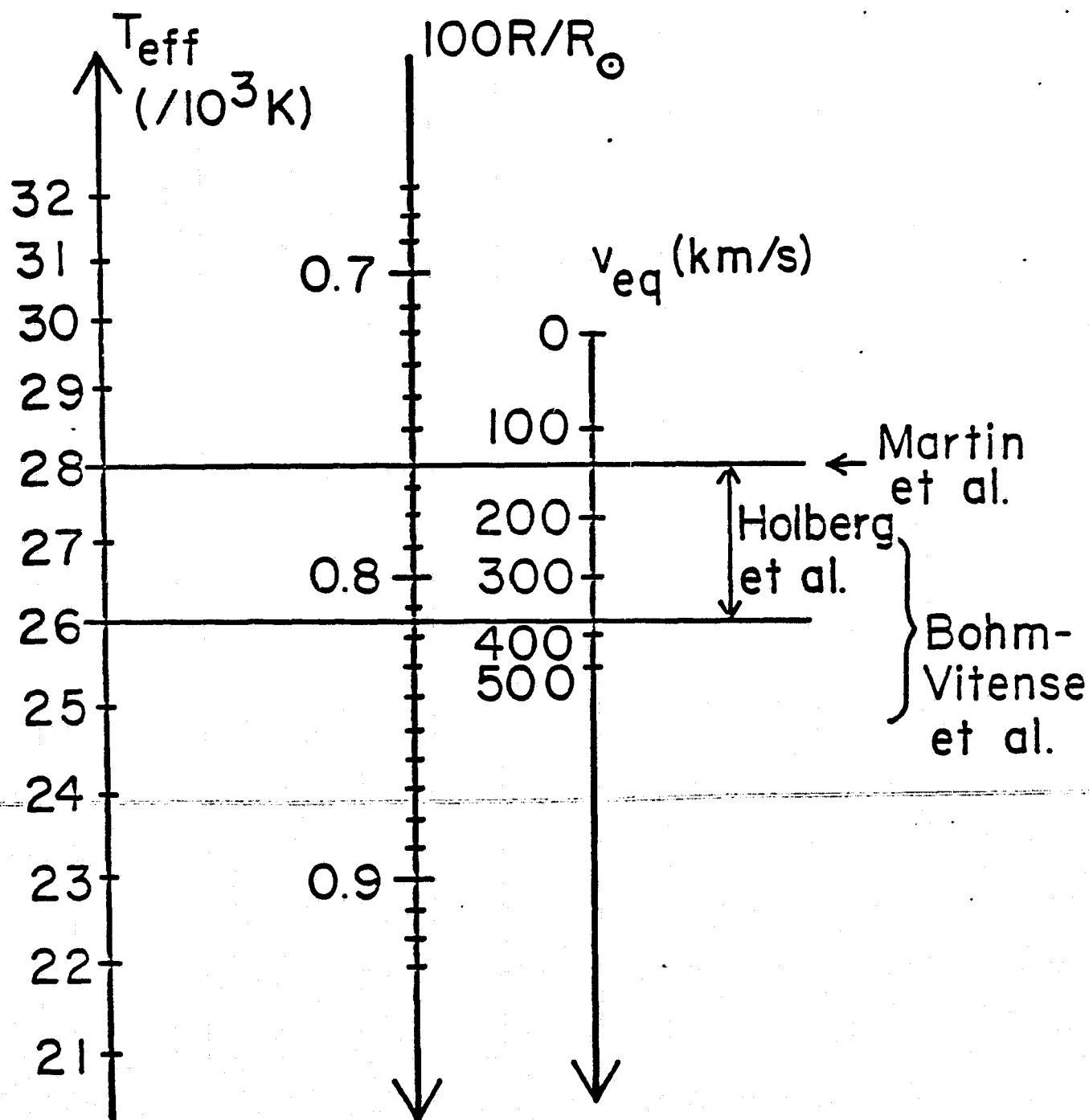
Fig.2. Nomogram showing how T_{eff}, radius and equatorial rotational velocity relate for a 1.05 M_0 white dwarf like Sirius B. The calculations assume a spherical homogenous mass distribution and use data from Hartwick and Ostriker, Gatewood and Gatewood and unpublished spectra of Sirius B from Greenstein, Oke and Shipman.

References.

Auer, L, H, and Shipman, H.L., 1977, *Ap. J. Lett.* 211, L103.

Bohlin, R.C., et al., 1980, *Astron. Astrophys,* 85, 1.

Bohlin, R.C., 1985, *NASA IUE Newsletter,* No. 26, 23.

Bohm-Vitense, E., Dettman, T. and Kapranidis, S. 1979, *Ap. J. Lett.,* 232, L189.

Gatewood, G.D., Gatewood, C.V., 1978, *Ap. J.,* 225, 191.

Greenstein, J.L., Oke, J.B. and Shipman, H.L., 1971, *Ap. J.,* 169, 563.

Holberg, J.B., Wesemael, F. and Hubeny, I., 1984, *Ap. J.,* 280, 679.

Koester, D. and Schonberner, D., 1986, *Astron. Astrophys,* 154, 125.

Martin, C., Basri, G. and Lampton, M., 1982, *Ap. J. Lett.,* 261, L81.

Mewe, R., et al., 1975, *Nature,* 256, 711.

Milkey, R.W. and Pilachowski, C.A., 1984, *PASP.,* 96, 821.

Ostriker, J.P. and Hartwick, F.D.A., 1968, *Ap. J.* 153, 797.

Rakos, K. D. and Havlen, R.J. 1977, *Astron. Astrophys.,* 61, 185.

Shipman, H.L., 1976, *Ap. J. Lett.,* 206, L67.

Shipman, H.L., 1979, *Ap. J.,* 228, 240.

Shipman, H.L., 1979b, *IAU Colloquium,* No. 53, 86.

Smith, B.A. and Terrile, R.J., 1984, *Science.* 226, 1421.

Wesemael, F., et al., 1980, *Ap. J. Supp. Ser.* 43, 159.